Mediterranean Tropical-Like Cyclones forecasts and analysis using the ECMWF Ensemble Forecasting System (IFS) with physical parameterizations perturbations

Miriam Saraceni[1], Lorenzo Silvestri[2], Peter Bechtold[3], and Paolina Bongioannini Cerlini[4]

[1,2]Department of Civil and Environmental Engineering, University of Perugia, Perugia, Italy
[4]Department of Physics and Geology, University of Perugia, Perugia, Italy
[3]European Centre for Medium-Range Weather Forecasts, Bonn, Germany

Correspondence: Miriam Saraceni (miriam.saraceni@unipg.it)

Abstract. Mediterranean Tropical-Like Cyclones, called "medicanes", present a multiscale nature and their track and intensity have been recognized as highly sensitive to large-scale atmospheric forcing and to diabatic heating as represented by the physical parameterizations in numerical weather prediction. Here, we analyse the structure and investigate the predictability of medicanes with the aid of the European Centre for Medium-Range Weather Forecast (ECMWF) Integrated Forecast
5 System (IFS) ensemble forecasting system with 25 perturbed members at 9 km horizontal resolution (compared to the 16 km operational resolution). The IFS ensemble system includes the representation of initial uncertainties from the ensemble data assimilation (EDA) and a recently developed uncertainty representation of the model physics with perturbed parameters (Stochastically Perturbed Parameterizations, SPP). The focus is on three medicanes, Ianos, Zorbas and Trixie that have been among the strongest in recent years. In particular, we have carried out separate ensemble simulations with initial perturbations,
10 full physics SPP, and with a reduced set of SPP, where only convection is perturbed to highlight the convective nature of medicanes. It is found that compared to the operational analysis and satellite rainfall data, the forecasts reproduce the tropical-like features of these cyclones. Furthermore, the SPP simulations compare to the initial condition perturbation ensemble, in terms of tracking, intensity, precipitation and more generally in terms of ensemble skill and spread. Moreover, the study confirms that similar processes are at play in the development of the investigated three medicanes, in that the predictability of these
15 cyclones is linked not only to the prediction of the precursor events (namely the deep cut-off low) but also to the interaction of the upper-level dynamically driven Potential Vorticity (PV) streamer with the tropospheric PV anomaly that is driven by surface heating and stratiform and convective condensational heating.

1 Introduction

The Mediterranean region is a small but geographically complex area characterized by sharp land and sea transitions and
20 surrounded by high mountain ranges. It is known for its frequent cyclogenesis. A small number of the intense cyclones that originate in the region present tropical-like features (Flaounas et al., 2022). They are a very significant phenomenon, due to their similarity with tropical cyclones, and while they are typically shorter-lived than North Atlantic hurricanes, they may exhibit

several tropical-like characteristics in their mature phase, such as a high degree of axial symmetry, a warm core, a tendency to weaken after making landfall, and a cloud-free "eye" at the center of the storm of mostly calm weather, as inferred from satel-

25 lite images. Such vortices are better known as Tropical-Like Cyclones or Mediterranean hurricanes (medicanes). Medicanes have been documented in the Mediterranean region since the beginning of the satellite era (Ernst and Matson, 1983) and have been associated with polar lows (Rasmussen and Zick, 1987). These storms pose a significant threat due to their intense winds, heavy rainfall, and associated flooding.

30 Medicanes features have been commonly observed in the literature (Cavicchia et al., 2014; Romero and Emanuel, 2013; Emanuel, 2005; Zhang et al., 2019; Miglietta and Rotunno, 2019). They occur very infrequently, with an average of about 1/2 events per year over the entire Mediterranean region. They are most commonly formed in the western Mediterranean and in the area between the Ionian Sea and the North African coast. Medicanes have a distinct seasonal pattern, with a peak at the start of winter, a significant number of events during fall, a few during spring, and very little activity in summer. As pointed out by

35 Miglietta and Rotunno (2019) they only have a lifespan of a few days due to the limited size of the Mediterranean Sea, which is their main source of energy. Furthermore, they only exhibit fully tropical characteristics for a short period, with extratropical features predominating for most of their lifetime (Miglietta and Rotunno, 2019).

Medicanes differ from other Mediterranean cyclones in the complexity of their formation and maintenance. Indeed, unlike

40 hurricanes, which develop in regions with near-zero baroclinicity and draw their energy from warm tropical oceans, medicanes form from pressure lows under moderate to strong baroclinicity, which is a typical condition of midlatitudes. The latter aspect leads to a low rate of occurrence, given that the environmental conditions of weak vertical wind shear, which are necessary for their development, are unusual (Nastos et al., 2018). The interaction between warm sea and cold air associated with a deep upper-level trough creates the necessary thermodynamic disequilibrium for these storms to develop a warm core (Emanuel,

45 2005; Miglietta and Rotunno, 2019). The type of mechanics that can be deemed responsible for the creation of a medicane in the Mediterranean is similar to the one responsible for the formation of tropical cyclones farther from the equator near the tropics (McTaggart-Cowan et al., 2015).

The development and maintenance of medicanes are the results of a synergy between synoptic-scale processes, which pro-

50 vide the necessary environment, and mesoscale processes such as deep convection and latent heat fluxes from the sea (Emanuel, 2005). Because of their small size, limited data availability, low frequency of occurrence (Cavicchia et al., 2014), and the complex geography of the Mediterranean region, studying and predicting medicanes is a challenge for numerical weather forecasting. For this reason, besides some climatological studies on medicanes, using synthetic production of tracks and 3D numerical simulation (Romero and Emanuel, 2013; Cavicchia et al., 2014) there is a higher rate of studies in the literature that

55 has been focused on modeling medicanes using convective permitting models, due to the fact that they can be more effective at reproducing the small-scale processes that contribute to medicane formation and maintenance (Davolio et al., 2009; Miglietta et al., 2011, 2013; Mazza et al., 2017; Cioni et al., 2016; Ricchi et al., 2019) rather than observational aspects (Pytharoulis

et al., 2000; Moscatello et al., 2008).

There have been relatively few studies that have analyzed medicanes using ensemble forecasts (Chaboureau et al., 2012; Mazza et al., 2017) and more specifically, by using the ECMWF ensemble forecasting system (Pantillon et al., 2013; Di Muzio et al., 2019; Portmann et al., 2020). Indeed, the ensemble forecast of ECMWF has proven to be a useful tool for predicting extreme weather events (Buizza and Hollingsworth, 2002; Buizza, 2008; Magnusson et al., 2015), for analyzing tropical cyclones (Torn and Cook, 2013) and their predictability (Munsell et al., 2013). Moreover, the model has demonstrated high predictive skill also for medicanes (Di Muzio et al., 2019). Pantillon et al. (2013) used ECMWF operational ensemble forecasts to study the predictability of a medicane in 2006 and found that they were more successful at consistently capturing early signals of its occurrence compared to ECMWF deterministic forecasts. Di Muzio et al. (2019), who used ECMWF ensemble forecasts to systematically analyze the predictability of medicanes, found that the ensemble members noted a marked drop in predictive skill beyond 5-7 lead days, indicating the existence of predictability barriers. Portmann et al. (2020) used ensemble forecasting to assess upstream uncertainties in the prediction of medicanes, finding also that the uncertainties were reduced with later initializations.

Research conducted on medicanes with ensemble forecasting has generally been carried out through the use of the perturbations to initial conditions only (Di Muzio et al., 2019; Portmann et al., 2020). However, an important part of the uncertainty associated with forecasting comes from uncertainty related to the physics of the model. For these reasons, this present study is concerned with ensemble forecasting that takes into account not only the uncertainty of initial conditions but also the uncertainty of model parameters. We present an assessment of the prediction of medicanes, with the use, not only of the Integrated Forecasting System (IFS) operational ensemble forecasting system at ECMWF, with initial conditions perturbation, but using also the physical parameterization perturbations, the Stochastically Perturbed Parameterizations (SPP) ensemble forecast. Indeed, this is a novel scheme of stochastic representation of model uncertainties which is still under development at ECMWF in order to replace the Stochastically Perturbed Parameterization Tendency scheme (SPPT) (Palmer et al., 2009). SPP has been found relevant in improving forecasts, specifically with ECMWF ensembles (Ollinaho et al., 2017a) and tropical cyclones. This new representation of uncertainties associated with model physics consists of a set of physical parameters in the model being perturbed (Ollinaho et al., 2017b). The use of this method is rising in the literature (Frogner et al., 2022) precisely because it allows the reproduction of uncertainty close to the actual source of error and maintains physical consistency, particularly with local conservation of energy and humidity (Lang et al., 2021).

Thus a comparison between three ensemble forecast experiments is set up. One ensemble is run with only initial condition perturbations, through the Ensemble Data Assimilation (EDA), one is run with the entire physical parameterizations perturbed and one is run with only the convective parameterization perturbed. The goal of this study is to determine whether these forecasts can accurately predict medicanes and if there are possible biases presented by the ensemble forecasts. The goal of the research is also to assess which of the perturbation experiments can capture the medicane more accurately and to understand

what physical processes, among the ones already studied in the literature, influence the forecast and how these are predicted by different ensembles.

95

Differently from Di Muzio et al. (2019), only three medicanes, among the strongest in recent years, were chosen: Ianos (September 15-20, 2020), Zorbas (September 27-31, 2018), and Trixie (October 28-November 1, 2016). The three medicanes have been selected because they are very different from each other, with Trixie being the weakest but also the longest lasting of the three (Di Muzio et al., 2019) and generally among the longest lasting medicanes, Zorbas one of the shortest-lived and
100   presenting high variability in predictability, as documented by Portmann et al. (2020) and Ianos one of the most intense medicanes ever observed, reaching category 2 hurricane status (Lagouvardos et al., 2022).

In section 2 the data and methods used are described, with an in-depth description of the ensemble forecast experiments carried out, a description of the SPP, and of the tracking method. In section 3 a brief overview of the three storms studied is
105   provided, highlighting their important characteristics. In section 4 the results are presented for the track position and intensity, precipitation, and thermal structure. In the final section 6, the results are discussed and the concluding remarks are given.

2   Data and Methods

In this section, a description of the methods and techniques used to analyze the medicanes with the ensemble forecast and the operational analysis with the ECMWF model Integrated Forecasting System (IFS), is given. Firstly, a description of the
110   Stochastically Perturbed Parameterizations ensemble forecast of IFS is provided, together with a brief description of the carried-out perturbation experiments. Secondly, the data, used to validate the simulation besides the operational analysis, are described. Finally, the tracking algorithm is described.

2.1   Ensemble Forecast Simulation

For this work, the ensemble forecast experiments with the ECMWF IFS (Cycle 47r3: ECMWF,(IFS Documentation CY47R3,
115   2021b)) and the ECMWF operational analysis have been used. Both the ensemble forecast and the operational analysis have a $\simeq$ 9 km horizontal grid spacing (TCo1279, for a more in-depth description of the horizontal grid, see Malardel et al. (2016)) and are run with 137 vertical levels. The forecasted period used in this work is 9 days. Three different sets of experiments have been conducted, all of them consisting of an 24-members ensemble. The ensemble forecasts are initialized, amounting to 3 initial dates, each day at 0000 UTC. For Ianos the three dates are the 15th, the 16th, and the 17th of September 2020,
120   for Zorbas the three dates are the 25th, the 26th, and the 27th of September 2018 and for Trixie, the three dates are the 25th, the 26th, and the 27th of October 2016. Regarding the physical parameterization, a detailed description can be found in the IFS documentation (IFS Documentation CY47R3, 2021a). The ensemble forecasts are coupled to the ECMWF Wave Model (ecWAM:(IFS Documentation CY47R3, 2021c)), to the Nucleus for European Modelling of the Ocean (NEMO) ocean model

(Mogensen et al., 2012) and the LIM2 sea-ice model (Goosse and Fichefet, 1999). The Different types of experiments that have been carried out are reported in Table 1.

Table 1. Description of the different ensemble forecast experiments

Experiment ID	Experiment Setup
INI	Initial perturbations only - no model uncertainty representation
$SPP - Conv$	No initial perturbations - convective parameterization uncertainty representation
SPP	No initial perturbations - physical parameterizations uncertainty representation

125

The first experiment is the ensemble forecast with initial condition perturbation only (INI experiment). This is done by adding perturbation to a 4D-Var (Rabier et al., 2000) analysis. The perturbations are constructed from an ensemble of 4D-Var data assimilations (Ensemble Data Assimilation, EDA, (Buizza et al., 2008)). The second and third sets of experiments are conducted by running the ensemble with SSP applied. In the former (SPP-Conv) only the convective parameterization

130 parameters are perturbed. In the latter (SPP), the whole physics parameterization, convection, radiation, clouds and large-scale precipitation and turbulence diffusion and sub-grid orography parameters are perturbed, as discussed below.

2.2 Stochastically Perturbed Parameterizations Ensemble

The Stochastically Perturbed Parameterizations scheme represents model uncertainty in numerical weather prediction by introducing stochastic perturbations into the physical parameterization schemes (Lang et al., 2021) as mentioned above. SPP

135 is a new scheme, aimed at replacing the currently used Stochastically Perturbed Parameterization Tendency scheme (SPPT) (Palmer et al., 2009) in the ECMWF ensemble forecast in June 2023. The new scheme, developed by Ollinaho et al. (2017b), following the work of Baker et al. (2014); Christensen et al. (2015), is based on applying perturbations directly to well-known poorly constrained parameters and variables within the parameterization schemes. This way the model uncertainty representation can be directly related to known sources of model uncertainties associated with specific processes. Thus, with the SPP,

140 some individual IFS parameters and variables are perturbed at each time step with in-space varying noise derived from in-time evolving 2D random number fields. The SPP scheme is designed such that it converges to the unperturbed (i.e. deterministic) forecast model in the limit of vanishing variance of the noise. The implementation of SPP allows simultaneous perturbations of up to 27 parameters and variables in the deterministic IFS parametrizations of turbulent diffusion (Köhler et al., 2011), subgrid orography (Beljaars et al., 2004), convection (Tiedtke, 1989; Bechtold et al., 2008), cloud processes and large-scale

145 precipitation (Tiedtke, 1993; Forbes et al., 2011), and radiation (ecRad, (Hogan and Bozzo, 2018)). These 27 parameters and variables are reported in Supplementary Tables 1 to 4, together with a thorough explanation. As mentioned above, the SPP perturbation is applied through a 2D random field generator. In its implementation, SPP uses a single scale with a decorrelation

length scale of 1,000 km and a decorrelation time of 3 days (Figure 1 of Lang et al. (2021)).

150 ## 2.3 Validation Data

In order to analyze the predictive skill of the ensemble, besides the operational analysis, the ensemble forecast perturbation experiments have been compared with the satellite-based, globally-gridded Global Precipitation Measurement (GPM) Integrated Multi-satellite Retrievals for GPM (IMERG) (Huffman et al., 2020). In GPM-IMERG, the retrievals from geostationary satellites are blended seamlessly with information from the passive microwave (PMW) sensors from low-orbit satellites. this

155 is done in order to provide for both a high accuracy and a high temporal (30 min) and spatial ($\simeq$ 10 km) resolution since the precipitation estimation based on only the PMW suffers from a low sampling rate. Furthermore, the data are also calibrated by using rain gauges at the ground base. In this research, the 24-hr accumulated precipitation values are used. The latter data are provided at the same resolution, 0.1°, of the ensemble simulation.

2.4 Cyclone tracking

160 The method described here has been used to evaluate the tracks for both operational analyses, used as verification and ensemble forecasts. The tracking method is based on Picornell et al. (2014) and Ragone et al. (2018). The algorithm is firstly aimed at finding the local minima of the sea level pressure field at each time step. Then, for each minimum, the gradient of the sea level pressure along eight principal directions (E, NE, N, NW, W, SW, S, SE) inside a circle of radius 200 km is computed. The computed gradient is then chosen to be lower than $5hPa/200km$ in at least 6 directions. After the minimum detection and

165 filtering via selection through seal level pressure gradient, a proximity condition is applied to construct the complete trajectory. Starting from the first time-step, each minimum is connected to the following one, at the following timestep, that respect the condition of being closer than $\Delta x = V \Delta t$, with $V = 50km/h$ and $\Delta t = 3h$. If this condition is met, the two consecutive minima are considered to belong to the same trajectory. This condition has been considered suitable and chosen according to the results of Ragone et al. (2018). Once the trajectories have been found, only the trajectories that last longer than 24 hours

170 and those that spend more than 12 hours over the sea are selected. Trajectories that spend less than half their duration over land or within 100 kilometers of the coast will be discarded.

3 Overview of the Storms

In this section, an overview of the three medicanes chosen is given. A brief analysis of the synoptic environment is provided, following the literature. A summary of the main features as retrieved by the analysis data: the storm duration, the period, the

175 region of occurrence and the asymmetry B, and upper-level thermal wind $-V_T^U$ (the last two parameters will be explained in the following sections) is provided in Table 2. The intensity (central pressure) and trajectory of each storm are shown in Figure 1 along with the ensemble tracks.

Table 2. Duration, region of occurrence, central pressure, CP, asymmetry parameter, B, and upper-level thermal wind from the operational analysis for each storm. The upper-level thermal wind, $-V_T^U$ and the thermal asymmetry parameter, B are taken from the Hart cyclones phase-space (Hart, 2003).

Storm	Region	Period	Duration (d)	CP (hPa)	B	$-V_T^U$
Ianos	SM	September 2020	7	994	0	73
Zorbas	SM	September/October 2018	5	993	4	39
Trixie	SM	October 2016	4	1009	2	38

*SM = Southern Mediterranean

3.1 Ianos

As the track suggests (Figure 1a) Ianos originated in the Gulf of Sidra after an upper-level cutoff low that formed on the 9th
of September moved eastward to the western Mediterranean and northern Africa. Then between the 14th-15th of September,
it emerged in the Gulf of Sidra, due to stratospheric dry intrusion with high vorticity values (Comellas Prat et al., 2021). This
process was also accompanied by an anomalous value of SST which was 1.5 °C higher than the normal (27-28 °C).

On the 16th of September, it intensified, and it moved to the Ionian sea, and then on the 17th of September, the system
showed a clear mid-level warm core, lining up with the cut-off low. Ianos obtained tropical characteristics at this point (CP =
994, B = 0, and $-V_T^U$ = 73). The analysis is capable to reproduce a value similar to the observed pressure minimum of 995 hPa
(Comellas Prat et al., 2021).

3.2 Zorbas

Zorbas formed at 12:00UTC on 27 September 2018 close to north Africa and then moved into the central Mediterranean,
turning eastward and moving over Greece into the Aegean Sea, where it finally decayed 4 d after its formation (Figure 1d).
Medicane Zorbas originated from a PV streamer created by the elongation of a large-scale trough in eastern Europe, which
reached the central Mediterranean Sea at 00:00UTC on 27 September 2018 (Portmann et al., 2020). This PV streamer broke
up at the time of cyclogenesis, resulting in the formation of a PV cutoff.

At the same time, as for Ianos, a large SST anomaly was taking place in the Gulf of Sidra, with similar intensity as in
the Ianos case. Zorbas cyclogenesis was also accompanied by a strong low-level advection of air with low virtual potential
temperature, Θ_e, across the Aegean sea. Then this air was substantially moistened by sea-surface fluxes as it traveled across
the Aegean Sea. One day after formation (28th of September), Zorbas presented a deep warm core (Table 2). After reaching the

200 state of the warm core when Zorbas reached Greece on 29 September 2018, this was sustained for the next few days. Zorbas reached its maximum intensity (observed 992 hPa), which is well captured by the analysis.

3.3 Trixie

Medicane Trixie formed on the 28th of October, as the consequence of a deep cut-off low which emerged on 26–27 October and moved from northern to southern Italy in the following days, triggering deep convective storms along the Italian west coast.

205 This PV anomaly crossed the Adriatic Sea on 28 October at O4:00 UTC (EUMETSAT analysis by Scott Bachmeier, Jochen Kerkmann, and Djordje Gencic) and then quickly moved to Sicily and approached Tunisia and Algeria. Then between the 26 and the 28 of October, the medicane started to develop in the area of the old PV anomaly. On the 29th of October, it deepened and moved to the east of Malta, then on the 30th of October, it moved eastward towards Greece (Figure 1g).

210 Trixie reached the warm core structure on the 30th of October. This is in line with observation (EUMETSTAT report). Eventually, it passed near Crete on the 31st of October. The most intense convective activity started after 12 h of 30 October 2016 and lasted until 31 October 2016 (Dafis et al., 2020). In the analysis, there was only a short intensification period evident and the minimum pressure was fluctuating between 1010 and 1014 hPa during the period from the 29th and the 30th of October, which might have been highly underestimated.

215

The three storms formed and developed in the same area, the Southern Mediterranean, in the Ionian and Aegean Seas. This region has one of the highest medicanes occurrences, as recognized in the literature (Cavicchia et al., 2014; Zhang et al., 2021). They occurred in the same period of the year, between September and November, the most frequent period for medicane occurrence (Romero and Emanuel, 2013). From Figure 1 it can be gathered that there are some differences in duration and intensity,

220 with Trixie being the longest-lasting of the three medicanes (in terms of the deepening phase) and Zorbas and Ianos being deeper than Trixie.

4 Results

This section examines the ensemble forecast experiments for certain aspects that are crucial for cyclones. The primary focus

225 is on the cyclone track, as it is largely influenced by large-scale processes and is therefore a direct reflection of the model's capability to reproduce multi-scale processes. The second feature under investigation is the cyclone's intensity, as measured by central pressure. This value is considered the most stable and robust metric for assessing the intensity of a cyclone on a global scale (Davis, 2018). Then the precipitation is analyzed. To conclude the analysis, the thermal structure and asymmetry have been evaluated by focusing on the asymmetry and the upper-level thermal wind parameters, belonging to the cyclone

230 phase-space theory of Hart (2003). Eventually, the vertical profiles of vorticity, divergence, and heating around the cyclone centre are investigated in comparison with the results of the above-mentioned parameters. Finally, the focus has been put on

the process behind cyclone formation and intensification to understand the results of the ensemble simulations.

4.1 Tracking

235 The ensemble tracking results are reported in Figure 1. As examples, the tracks starting from the 16th of September are shown for Ianos, the ones starting from the 27th of September are shown for Zorbas, and the ones starting from the 27th of October are shown for Trixie.
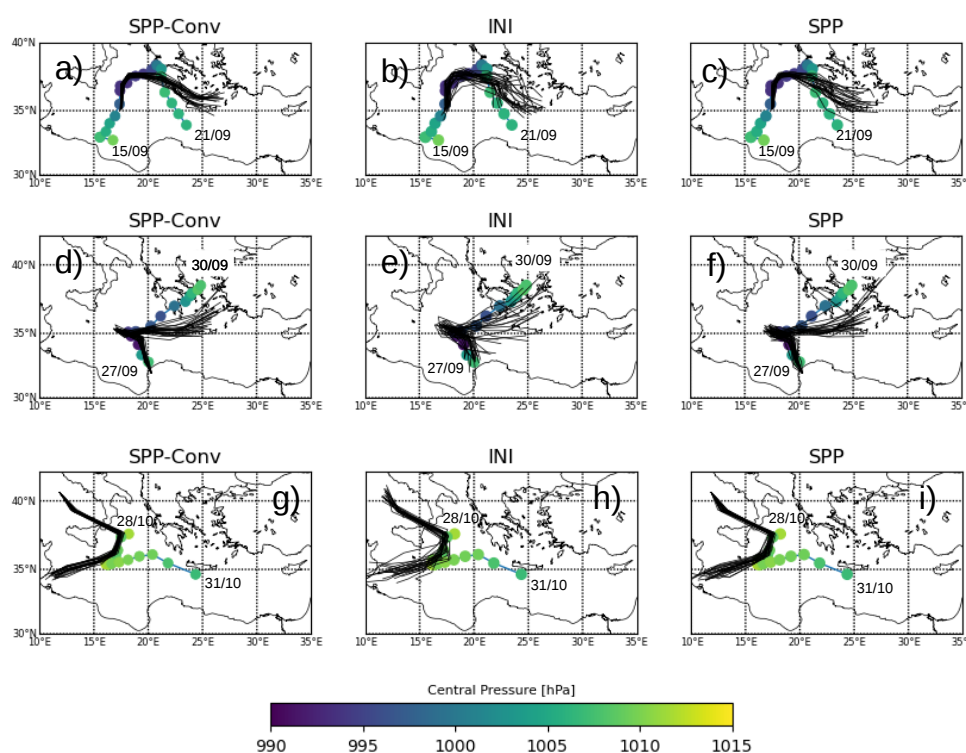
Figure 1. Track of the three storms for the operational analysis as reference track and for the ensemble members belonging to each experiment (SPP-Conv on the first column, INI on the second column and SPP on the third column) for the three storms, Ianos in a, b and c, Zorbas in d, e and f and Trixie in g, h and i. As background the operation analysis is reported with the colours representing the intensity, meaning the central pressure in hPa. For Ianos the experiments starting on the 16/09 have been chosen, for Zorbas the ones starting on the 27/09 and for Trixie the ones starting from the 27/10.

By looking at Figure 1a to c and Figure1d to f the ensemble tracks follow sensibly the references for Ianos and for Zorbas.
240 On the contrary for Trixie, the tracking, which starts one day prior to the starting date of the reference track (starting on the 28th) follows the track until the 29th early hours (Figure 1g to i) when it diverges and ends up in North Africa, underlying a

missed forecast. This is consistent also for earlier starting dates (the 25th and the 26th) with a greater error in terms of initial position (not shown). Figure 1 shows that, as expected, the simulations with initial conditions perturbations present usually more spread in the initial position. However, the spread at later stages in the simulation seems to be similar for both the INI experiment and the two experiments with the perturbation on the physics, SPP, and SPP-Conv.

For Ianos the 16th of September was chosen as an example, but the behavior for the three starting dates is quite similar, with them being able to reproduce the trajectory quite well for the first days and the error increasing with time. The latter is computed as the root mean squared error between the ensemble mean track and the reference track. It never exceeds 300 km (not shown) and up to 48 hours is always below 100 km (not shown). The error values are similar in all three experiments, but slightly lower for the INI experiment. In the case of Zorbas and Trixie, since the starting dates are earlier than when the reference track starts, the earlier the simulations start, the more uncertainty there is with respect to the starting position, thus the more spread. In Figure 1 the latest starting dates simulations are shown for both cyclones. For Zorbas, starting from the 27th, the obtained tracks are following the reference with a small error at least for the first days, which is anyway always under 300 km, at later stages. As in the case of Ianos the error committed by the three experiments is similar. For Trixie, the error, regarding the 27th, the last starting date shown in Figure 1g, h and i, goes up to 700/800 km for the three experiments.

The tracking results shown in Figure 1 are mirrored by the ensemble spread and the relationship between the spread and the error presented in Figure 2 and Figure 3 respectively. Following the approach of Hamill et al. (2011), the spread of the ensemble for a single cyclone ensemble forecast at a given forecast time is defined as:

$$S_l(t) = \frac{1}{n} \sum_{i=1}^{n} D_i \qquad (1)$$

where D_i denotes the great-circle distance of the ith ensemble member position of the cyclone from the ensemble mean cyclone position. The total number of ensemble members used for the calculation is 24 and the spread has been computed for each starting date (3 dates for each medicane). The results, reported in Figure 2, regard the same starting date as in Figure 1, thus for Ianos is the 16th of September, for Zorbas the 27th of September, and for Trixie the 27th of October, as also representative of the spread of the other starting dates. It is shown that for the three cyclones the INI experiment shows the largest mean track spread (Figure 2a, b and c). Then the spread for the SPP and the SPP-Conv ensembles spread is comparable, reaching similar valued to the INI ensemble at the end of the simulation. Ianos ans Zorbas present less spread than Trixie upon initialization for the INI experiment in particular. This might be due to the fact that for Trixie, which analysis track starts on the 28th of October (Figure 1g to 1i) a great uncertainty in the initial position of the track exists.

When looking at the spread-skill relationship (Figure 3), measured by the ratio of the ensemble spread and the root mean squared error between the ensemble mean track and the reference track, it can be said that as mentioned before the error is always greater than the ensemble spread and they are only comparable in the first hours of simulations (20h to 40h) when the spread/skill values are nearer to 1. Both the SPP and the SPP-Conv are usually more under-dispersed than the INI experiment in all three cases, but the three experiments perform generally in the same way, with the INI experiment presenting lower error after the second day for Ianos and Zorbas, but behaving similarly in Trixie.
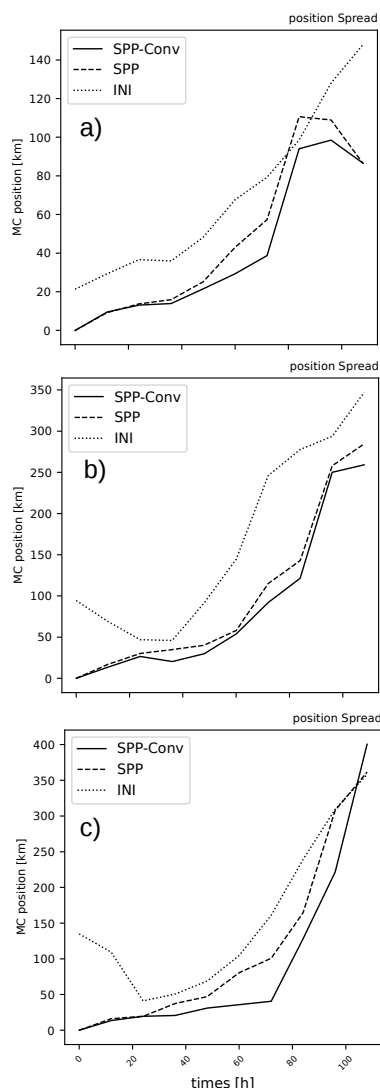
Figure 2. Mean ensemble spread of the medicanes track for each ensemble perturbation experiment for Ianos (a), Zorbas (b) and Trixie (c). The track spread is computed as described in Eq. 1 and is reported in km. For Ianos the experiments starting on the 16/09 have been chosen, for Zorbas the ones starting on the 27/09 and for Trixie the ones starting from the 27/10, in order to be consistent with the ensemble tracks shown in Figure 1

At later forecast steps, Trixie is the cyclone with the highest spread for all three perturbations compared to Ianos and Zorbas. By looking at the general spread trends, the INI experiment spread is highest at initialization, as also seen in Lang et al. (2012), since the EDA perturbations (INI experiment) are associated with a shift and intensification/weakening of the cyclone. Even considering the case-to-case variability, in terms of the spread of the track, the SPP-Conv experiment is the one with consistently

280 less spread for all the cyclones. The low error values obtained by Ianos and Zorbas, compared to the values reached in the case

of Trixie ($\geq$ 800 km), make it not only the medicane with the largest spread but also, the most significant error. Indeed, it has

been verified that this particular simulated cyclone diverges from the analysis track. The Trixie simulation track is probably a

result of the ensemble forecast not capturing properly the processes connected to the cyclogenesis, but it can also be related to

the simulations starting too early before the medicane appearance. This is an aspect also recognized by (Di Muzio et al., 2019)

285 in the simulation of these events.

It has to be noted here, that both experiments with SPP, and specifically the SPP-Conv one, manage to produce a spread
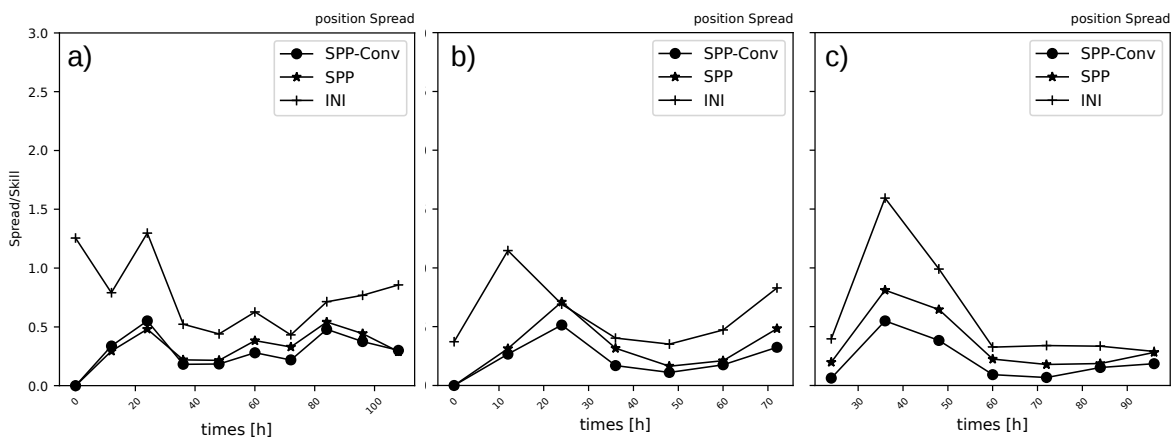
Figure 3. Ensemble Spread/skill relationship for each ensemble perturbation experiment for Ianos (a), Zorbas (b) and Trixie (c). The spread is computed as in Eq. 1 and the skill is the root mean squared error between the ensemble mean and the analysis tracks. For Ianos the experiments starting on the 16/09 have been chosen, for Zorbas the ones starting on the 27/09 and for Trixie the ones starting from the 27/10, in order to be consistent with the ensemble tracks shown in Figure 1.

comparable to the one produced by the initial condition perturbation. Similar results have been found in Lang et al. (2012). These results underline the importance of the role of convection and convective heating in explaining the source of uncertainty in the development of these cyclones.

290 **4.2 Intensity**

The other important aspect investigated is the intensity of the cyclones analyzed. The intensity is assessed by studying the minimum core pressure at the cyclone position.

The development of the core pressure with the simulations is reported in Figure 4 where the mean sea level pressure at the centre of the cyclone (Minimum Core Pressure in Figure 4) is shown, with the ensemble mean, the 25%-75% percentile and

295 the 5%-95% percentile compared to the analysis for the three ensemble experiment for chosen starting dates, as an example. For Ianos there is an overestimation of the deepening of the cyclone (Figure 4a, d and g), with a temporal shift of one day, compared to the analysis, which is consistent in all three experiments. For Zorbas the minimum pressure is underestimated
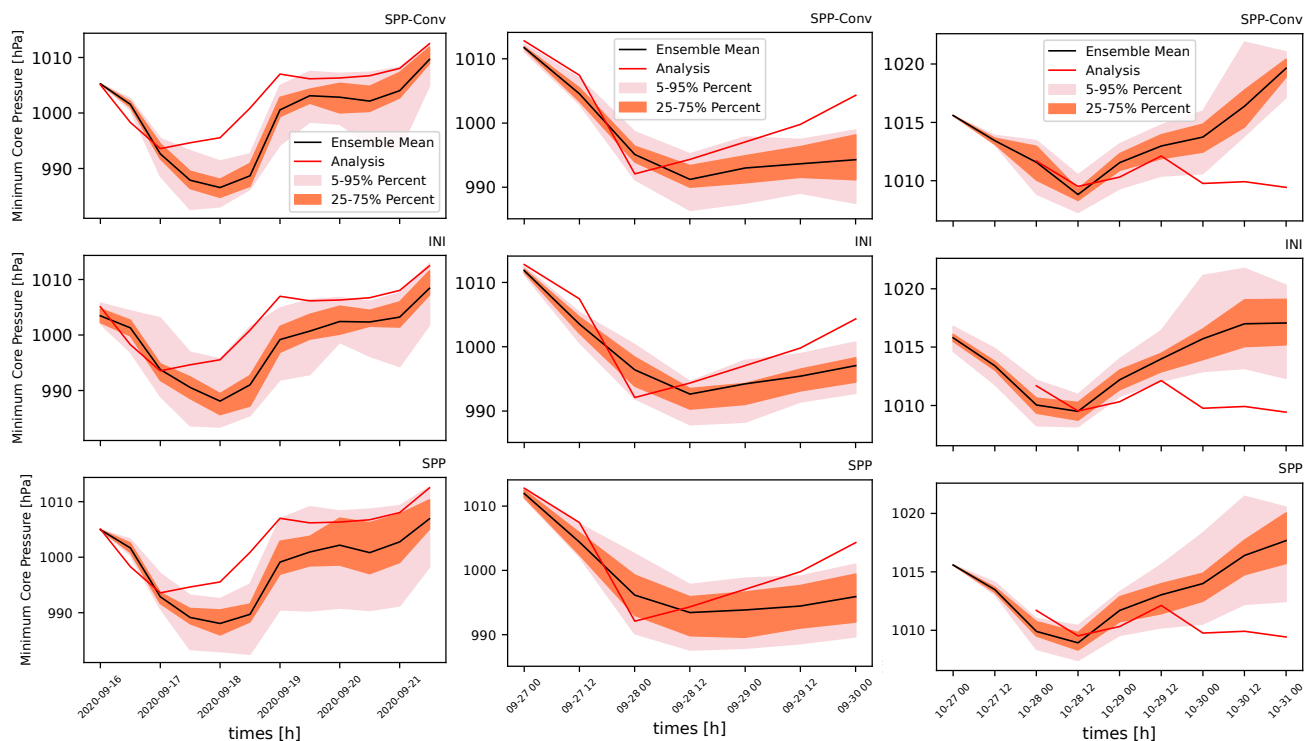
Figure 4. Analysis of the mean seal level central pressure, for Ianos in the first column, for Zorbas in the second column, and for Trixie in the third column. The plots show the ensemble members' development throughout the simulation. In each Figure the ensemble mean is reported in black, the operational analysis is reported in red and the two shaded areas represent the 25-75 % percentile and the 9-95 % percentile. The SPP-Conv experiment is reported for each medicane in Figures (a), (b), and (c). The INI experiment is reported in Figures (d), (e) and (f) and the SPP experiment in Figures (g), (h) and (i). in (b), and the SPP experiment in (c).

only in the case of the SPP-Conv experiment, however, there is a shift of 12 hours compared to the analysis in the three experiments (Figure 4b, e and h). In the case of Trixie, there is an underestimation (Figure 4c, f and i) and the ensemble exper-
300   iments are not able to capture the entire development of the cyclone pressure (especially the second deepening around the 30th).

In all three cyclones, the spread is slightly larger for the SPP and the SPP-Conv experiment compared to the INI one, however the reference analysis is included in the ensemble spread of the latter experiments compared to what happens with the SPP experiments, at least in the initial timesteps. This is particularly true for Ianos (Figure 4a, d and g). For Zorbas, the deepening
305   of the pressure is slightly better captured by the SPP ensembles (Figure 4b and h). As pointed out before, there is a shift of the minimum pressure of 12 to 24 hours compared to the analysis. For Ianos this is also present in the simulation starting on the 15th but is absent when starting the simulation on the 17th. This is due to the improved initial conditions with the forecast start date closer to the occurrence. The same can be said for Zorbas. As for Trixie, besides the first deepening happening on

the 28th of October, which is well captured by all experiments, the second minimum, which is the deepest, is not captured by

310   any of the members of every experiment, even if starting from the 27th of October (the last starting date). In general, there is

an underestimation of the pressure minimum and the trend up to the 29th is captured better by the SPP experiment (Figure 4i).

4.3   Precipitation

The precipitation field has also been analyzed and verified against observation. The verification field is chosen to be the pre-

cipitation, as in Vich et al. (2011); Montani et al. (2011). Matching the forecast and the verifying data is made difficult by

315   the irregularly spaced ground network of observations and by the fact that precipitation is not a continuous field, thus a point-

to-point verification presents several problems and is guaranteed by using satellite data. Thus, in this work observations from

satellites, specifically the above-discussed Integrated Multi-satellite Retrievals for GPM (GPM-IMERG), are used.

The precipitation structure of the three medicanes, in terms of intensity and position, is similar to what is observed in tropical

320   cyclones (Zhang et al., 2021, 2019). Indeed, there are similarities in their rainfall structures and those for Mediterranean

cyclones (Flaounas et al., 2018) where most precipitation associated with medicanes is concentrated to the northeast side of

the cyclone centre, as is shown in Figure 5 for the three cyclones. For the three cyclone, the ensemble mean of the last starting

date is shown. For each cyclone, the daily accumulation on the day of the "tropical-like" phase is shown in Figure 5. For Ianos

is the 17th of September, for Zorbas is the 28th of September, and for Trixie is the 28th of October. The daily accumulation

325   values from the ensemble forecast experiments are comparable, within the error to the observed values only regarding Ianos.

In general, the maximum is better captured by the SPP experiments for Ianos (Figure 5a and c), while for Zorbas and Trixie

this is true for the INI and SPP-Conv experiments (Figures 5e, f, i and l). The standard deviation of each ensemble experiment

reveals that there is higher uncertainty related to the higher values of the precipitation distribution (Supplementary Figure S1).

This is consistent for all three cyclones. There is little difference between the SPP-Conv and the SPP experiment in terms of

330   precipitation distribution. This mirrors what was shown in Figure 4.

The positioning of the maximum precipitation in the presented distributions (Figure 5), in general, is in accordance with the

observed GPM-IMERG distribution. However, there are some other secondary maximums in the distribution that are not well

captured, for all three cyclones. The daily accumulated precipitation shown in Figure 5 belongs to the simulations with the

335   latest starting date, where the maximum precipitation is better captured. Indeed, the error in the simulated ensemble mean pre-

cipitation maximum compared to the observation is decreasing with the forecast start date closer to the medicane occurrence.

This is specifically true for Ianos and Zorbas (as it is shown in Supplementary Figure S2), while for Trixie, the maximum is

equally underestimated. For Trixie, the simulation is not able to capture the intensity of the precipitation. This is linked to the

absence of the deepening of the cyclone and the precipitation starts to decrease sensibly after the 28th. This is seen within all

340   the starting dates. In order to evaluate the whole performance of the ensemble some probabilistic precipitation thresholds have

been chosen from 1 to 150 mm, and all the ensemble members have been considered. Following the cyclone position at each

timestep, an area of 500 km^2 around the cyclone centre has been considered for evaluation. The analysis has been carried out

mm/day   mm/day   mm/day   mm/day
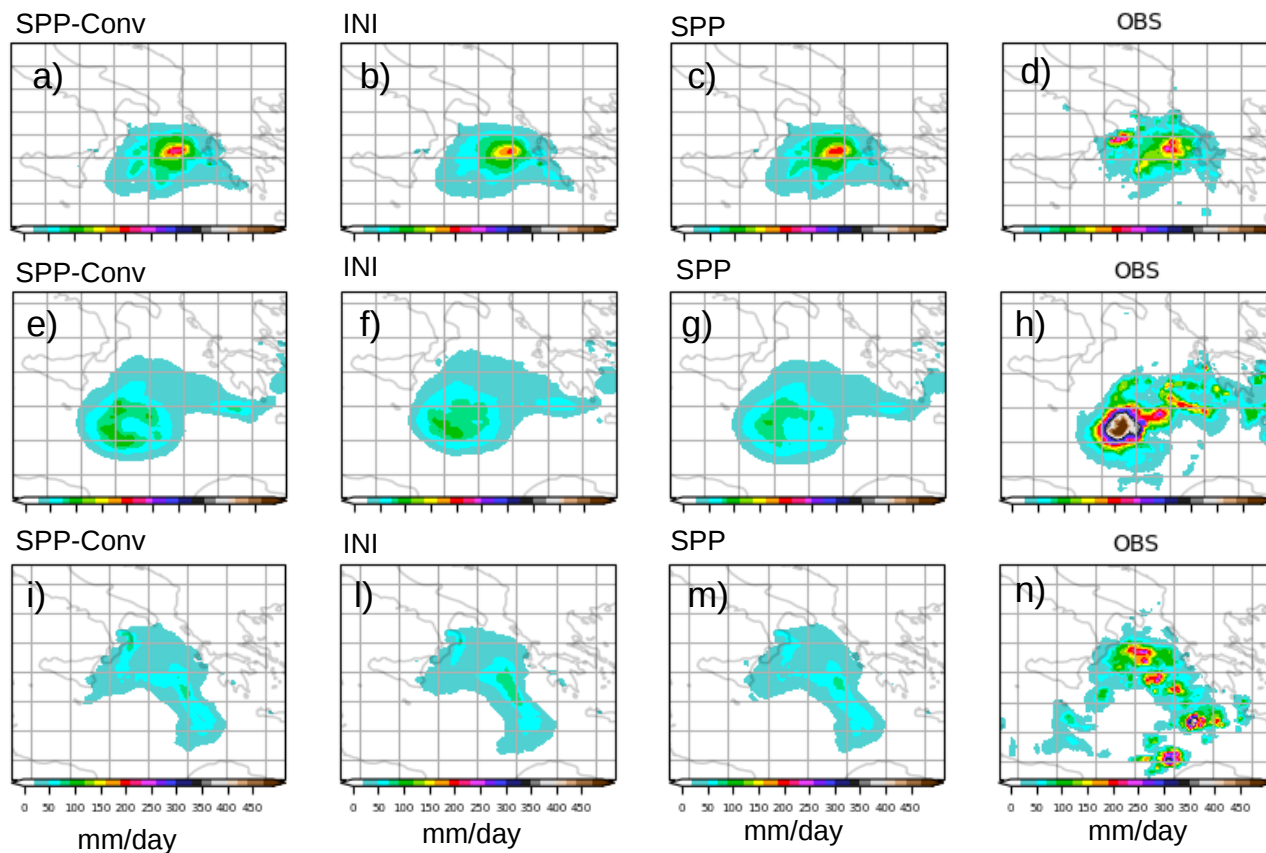
Figure 5. Daily accumulated precipitation (mm/day) for the three ensemble experiments ensemble means compared to the satellite observation GPM-IMERG. For Ianos the 17th is shown in Figures (a), (b) (c) and (d). For Zorbas the 28th is shown in Figures (e), (f) (g) and (h). For Trixie the 28th is shown in Figures (i), (l) (m) and (n). the SPP-Conv ensemble forecast accumulated precipitation is reported in the first column, the SPP ensemble in the second column, the INI ensemble in the third column and the observations in the fourth column. For Ianos the experiments starting on the 17th is shown, for Zorbas the ones starting on the 27th and for Trixie the ones starting from the 27th.

using many verification measures, following the literature (Montani et al., 2011; Marsigli et al., 2008; Vich et al., 2011; Buizza et al., 1999). A brief description of these measures is given in the Supplementary Information. All the verification results have
345   been calculated for the entire simulation period, according to their starting date.

Starting with the Brier Score (BS) (Brier et al., 1950) it can be said that the three ensemble experiments for the three medicanes are generally better than the control forecast at simulating the observed precipitation at all thresholds, as it is shown in Figure 6. Indeed, BS indicates the root mean squared error between the observed and the forecast probabilities, thus the
350   lower the better, and in our study, the BS is higher in the control run than in the three perturbations runs.
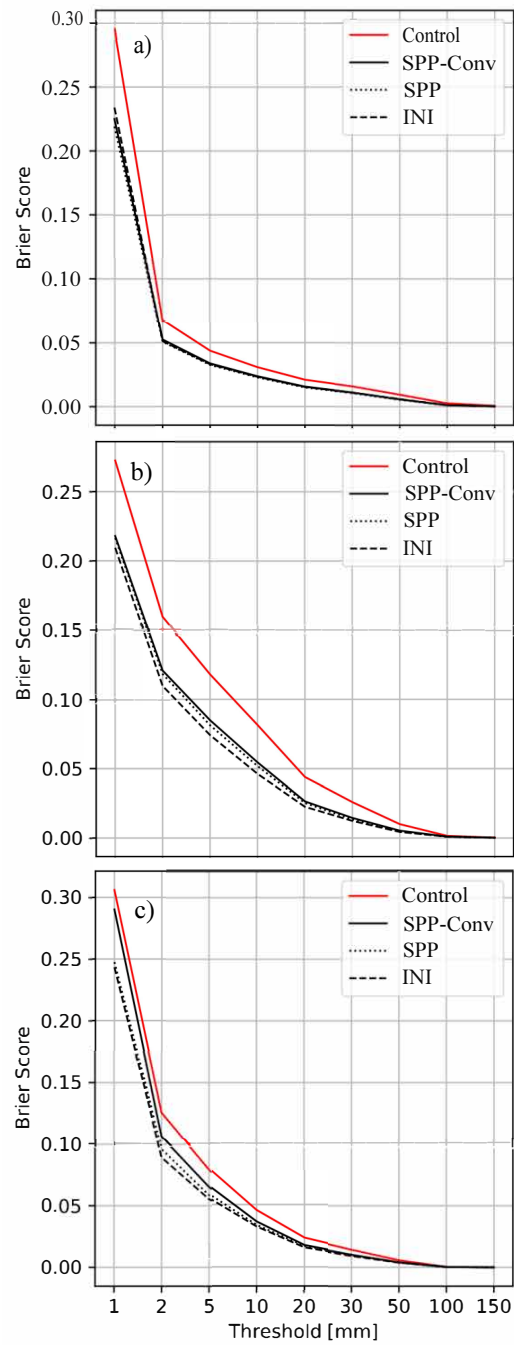
Figure 6. Brier score for the SPP-Conv ensemble forecast experiment, for the SPP ensemble forecast experiment, and for the INI ensemble experiment for Ianos (a), Zorbas (b) and Trixie (c).

For Ianos, which presents the lowest values, the three perturbation ensembles are almost indistinguishable (Figure 6a), while for both Zorbas and Trixie the perturbation experiment SPP-Conv has a slightly higher value than the SPP and the INI experiment (Figure 6b and 6c). The difference between the three experiments decreases with increasing thresholds, and in general, the improvement of the ensemble experiments compared to the control run decreases for extreme events when the
355 Brier score tends to zero as the events become increasingly rare. To further analyze the respective skill of the three ensemble experiments, the Relative Operating Curve (ROC) has been computed as a measure of forecast resolution. In general, for precipitation from 2 to 50 mm the ROC reached values between 0.7 and 0.8 for Ianos and Zorbas (not shown) which indicates a useful forecast (Buizza et al., 1999). The difficulties in predicting extreme precipitation, values over 50 mm may be probably due to the grid length of 9 km.

360 **4.4 Thermal structure and asymmetry**

To complete the analysis of these three storms, the thermal structure, and the thermal asymmetry have been investigated. The chosen parameter to quantify the latter has been recognized in the upper-level thermal wind, $-V_T^U$, which is considered to be a relevant parameter in distinguishing tropical-like cyclones from fully baroclinic cyclones (Mazza et al., 2017), and secondly on the thermal asymmetry, B. These parameters belong to the theory of the three-dimensional cyclone phase space introduced by
365 Hart (2003). There, the thermal asymmetry is defined as the storm-motion-relative 900–600 hPa thickness asymmetry across the cyclone within its radius:

$$B = (\overline{Z_{600\,hPa} - Z_{900\,hPa}}|_R - \overline{Z_{600\,hPa} - Z_{900\,hPa}}|_L) \tag{2}$$

where Z is the geopotential height, R indicates the right of current storm motion, L indicates the left of storm motion, and the overbar indicates the areal mean over a semicircle around the cyclone centre.

370

Instead, the cyclone's upper-level thermal structure (i.e., its cold or warm core) is indicated by $-V_T^U$. If it attains a positive sign, the cyclone attains an upper-level warm core. Indeed the $-V_T^U$ is defined as:

$$-|V_T^U| = \frac{\partial(\Delta Z)}{\partial ln(p)}\Big|_{600\,hPa}^{300\,hPa} \tag{3}$$

The two pressure levels have been changed from 600 hPa to 700 hPa and from 300 hPa to 400 hPa due to the lower height of
375 the tropopause in the midlatitudes with respect to the tropics (Picornell et al., 2014). These values are computed within a 200 km radius around the detected cyclone center. In the Hart (2003) formulation, this radius was chosen to be 500 km, but given the smaller size of medicanes compared to tropical cyclones (Miglietta et al., 2013), the radius used in this study is smaller, 200 km. The choice to consider important only the upper-level structure, compared to the lower-level (thus using also the lower-level thermal wind $-V_T^L$) is because its positive value can characterize not only medicanes but also extratropical cyclones with
380 warm seclusion (Hart, 2003). In the case of the thermal asymmetry, the threshold value of $B = 10\,m$ has been determined by analyzing ECMWF reanalyses ERA40 at $1.125°$ of the resolution, from which no major hurricane (winds of greater than 210 km/h) had associated with it a value of B that exceeded 10 m (Hart and Evans, 2001). Even if the threshold value of B has been

originally determined for larger tropical/extratropical cyclones, previous studies have shown that such value is also useful in the case of medicanes (Miglietta et al., 2011).

385

The Hart parameters, $-V_T^U$ and B, are analyzed in Figure 7. The focus has been put on the values where the deepening of the cyclone occurred in the observation, thus the values in Table 2 are reported as references in Figure 7. The violin plots of the forecast distribution for each experiment at different starting dates are shown with the median (white dot) and the interquartile range (gray bar). The sections at the sides of each violin plot represent the kernel density estimation to show the distribution shape of the data (wider sections of the violin plot represent a higher probability that members of the population will take on the given value; the skinnier sections represent a lower probability). The choice for the violin plot has been made because, unlike a box plot that can only show summary statistics, violin plots depict summary statistics and the density of each variable In Figure 7 only the SPP-Conv and the INI experiments are shown for comparison, because the results of the SPP experiments, as already pointed out above, are very similar to the one obtained by the SPP-Conv.

395

The forecast distribution in the three ensemble experiments presents different behaviors compared with the analysis reference value (ref in Figures 7) and with the starting date in the three experiments. Generally, the three ensemble experiments can reproduce the thermal structure of the storms, showing in some cases decreased spread with forecast start date closer to the occurrence, probably linked to the fact that these starting dates coincide with the period in which the cyclone had already developed (see Figures 7a and c for Ianos) and that the appearance of a symmetrical storm can benefit from improved initial conditions Di Muzio et al. (2019). This behavior is consistent for all three perturbation experiments.

The simulations of Ianos show a reduced spread with later starting dates accompanied by the distribution value approaching the analysis value, for the thermal wind (Figures 7a and c), and the thermal asymmetry (Figures 7b and d). Specifically, for the thermal asymmetry B, this makes the spread of the ensemble to be included below the threshold of 10 m which would define the system as a frontal system rather than a non-frontal one (Miglietta et al., 2013), thus showing a better performance in reproducing the tropical-like phase of medicanes. This is true for both experimetns, INI and SPP-Conv, and also for Zorbas and Trixie. In the case of Zorbas, there is a usually smaller spread for the last starting date only regarding the thermal wind (Figures 7e and g). Instead, there is a comparable spread for the thermal asymmetry, especially regarding the INI experiment (Figure 7h). However, the forecast distribution of both experiments contains the reference analysis values for both the thermal wind and the thermal asymmetry (Figure 7e to h). In Trixie, the spread is comparable between the starting dates for the thermal asymmetry parameter and thermal wind (Figures7i to n). There is also a consistent underestimation of the thermal wind (with median values of $-V_T^U$ around -25 to -50), in all three ensemble experiments. The forecast distribution is closer to the analysis values ($-V_T^U = 39$) for the third starting date, for both ensemble experiments, as shown in Figures 7i and m. This underestimation of the upper-level thermal wind means that a warm core was never reached in the ensemble forecast experiments, as it will be explored in the following sections.
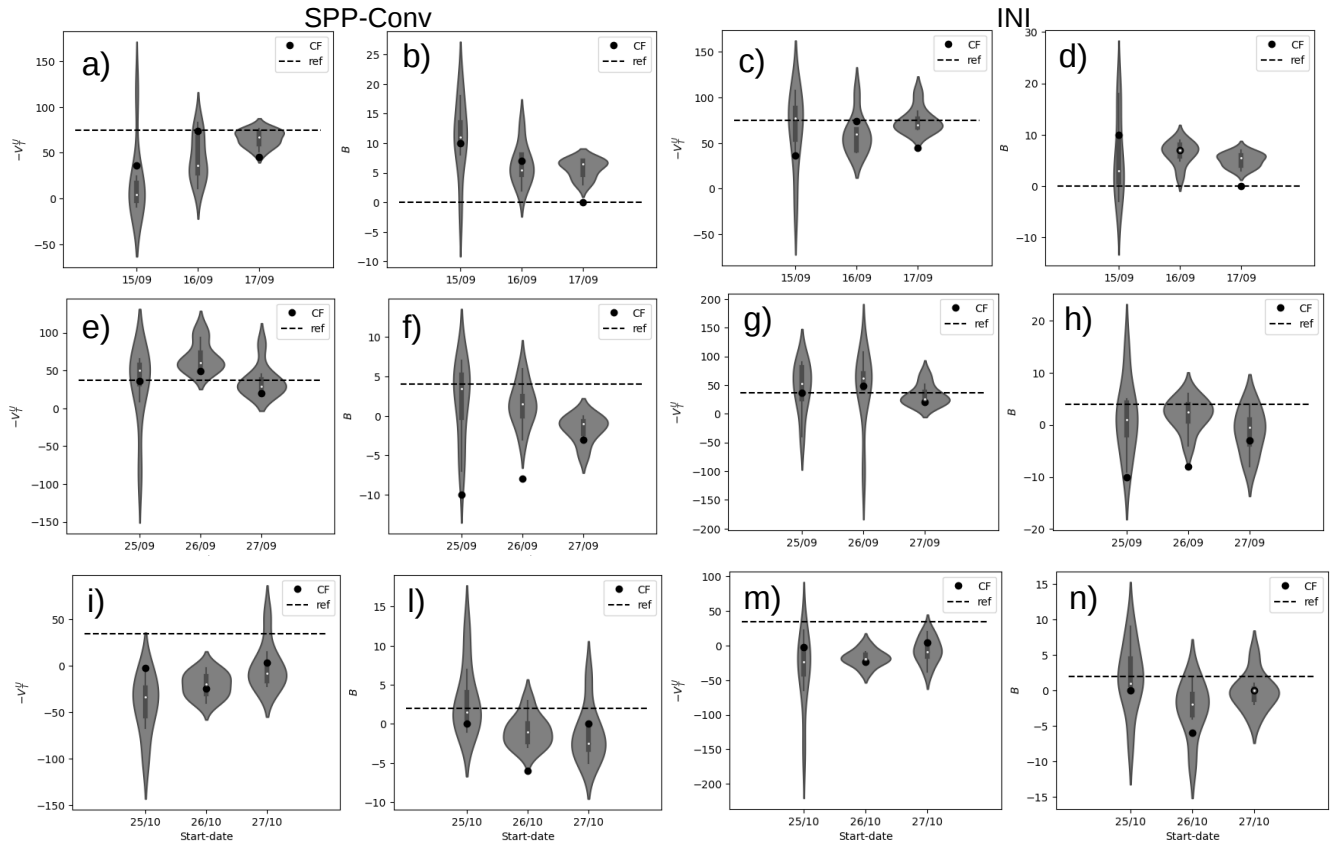
Figure 7. Ensemble forecasts violin plots of thermal wind, $-V_T^U$, and thermal symmetry, B, for each starting date for Ianos in Figures (a) and (b) for the SPP-Conv ensemble forecast and in Figures (c) and (d) for the INI ensemble forecast, for Zorbas in Figures (e) and (f) for the SPP-Conv ensemble forecast and in Figures (g) and (h) for the INI ensemble forecast and for Trixie in Figures (i) and (l) for the SPP-Conv ensemble forecast and in Figures (m) and (n) for the INI ensemble forecast. The violin plot is a hybrid of a box plot and a kernel density plot, which shows peaks in the data. The white dot represents the median, the thick gray bar in the center represents the interquartile range (25th-75th) and the thin gray line represents the rest of the distribution. On each side of the gray line is a kernel density estimation to show the distribution shape of the data.

4.5 Tropical-like phase

A more in-depth analysis of the tropical-like phase of these Mediterranean cyclones is carried out by means of the divergence
420 (s^{-1}), vorticity (s^{-1}), and time tendencies of the temperature (K/s) and specific humidity ($g/kg/s$) profiles around the cyclone centre (within a radius of 200 km). The latter profiles are reported in Figure 8 to 10 for the SPP-Conv experiment as an example and in there the temperature and humidity tendency are reported as Q1 for temperature and Q2 for humidity as is usual in the literature (Grabowski et al., 1999; Yanai et al., 1973), where $Q1 = \frac{dT}{dt}$ and $Q2 = -\frac{L_v}{c_P}\frac{dq}{dt}$. For data volume, the analysis of the

ensembles has been reduced to consider a subset of 8 members, instead of 24.

425   In the case of Ianos, which becomes a warm core cyclone on the 17th of September (Figure 8c and d at 00 UTC), the Q1 signals that the warming is happening at 500 hPa and it has deepened from 12 hours earlier, on the 16th of September (Figure 8a at 12 UTC), where the maximum is located at 600 hPa. This indicates a deepening warm core. Q2 signals the presence of diabatic heating by condensation throughout the mid-troposphere, which is increasing in the tropical phase. The tropical-like phase is accompanied by strong divergence above 400 hPa and convergence below 800 hPa (Figure 8b and d). The vorticity increases in

430 the mid and upper troposphere on the 17th (Figure 8d) compared to the 12 hours prior. The warm core is sustained for another day and the cyclone starts disappearing around the 19th. By the 20th (Figure 8e and f) the cyclone is dying out, with almost no divergence and no convective warming.

   Similar behavior can be observed for Zorbas in Figure 9. The divergence increases above 400 hPa in the tropical phase,

435 around the 28th of September (Figure 9d at 12 UTC) compared to the previous day (Figure 9a and b on the 27th at 12 UTC). The same can be said for the vorticity in the upper and mid-troposphere. The warming intensifies and moves to the upper troposphere (Q1 and Q2 profiles in Figure 9a and c). After two days of "tropicalization" the cyclones starts to weaken and by the 1st of October (Figure 9e and f) the divergence is almost null and the warming is decreased. The results obtained here resemble the ones obtained also for tropical cyclones (Geetha and Balachandran, 2016; Lin and Qian, 2019) while intensification

440 is occurring. For this reason, it can be said that Ianos and Zorbas actually undergo a tropical phase. There, the heating that is observed in the simulation is caused by the release of latent heat in the condensation process inside clouds, as also confirmed by observations for Ianos (Zimbo et al., 2022).

   For Trixie instead, the warm core state is never reached. As said before this cyclone is the weakest and it can intensify

445 only on the 28th in the ensemble simulations (Figure 10c and d at 00 UTC). The convective heating represented by a positive Q1 and Q2 is weaker compared to the other cyclones (Figure 8 and 9) and the maximum is located in the mid-troposphere, signaling a shallow warm core. The divergence, which is increasing compared to the previous 12 hours (Figure 10b and d) is not accompanied by an increase in vorticity and it starts at mid-troposphere. In general, this phase, which does not correspond to a warm core, mirroring the results shown in Figure 7, is reached only in the 28th, but on the 30th, when Trixie is supposed

450 to become a tropical-like cyclone (Dafis et al., 2020), is absent. The profiles regarding the latter day are shown in Figure 10e and f. The warming is weak and there is no divergence.

   By comparing Figure 8c, Figure 9c and Figure 10c it can be said that the spread is lower for Ianos, meaning lower uncertainty on the nature of the medicane compared to Trixie and Zorbas. The spread in Zorbas is reduced by forecast start date closer to

455 occurrence (not shown) in favor of the higher values for Q1 and Q2 (shown in Figure 9c which represents the profiles of the latest starting date) mirroring Figure 7e and g. Trixie presents the highest spread regarding the warming, mirroring the results of Figure 7e to 7n.
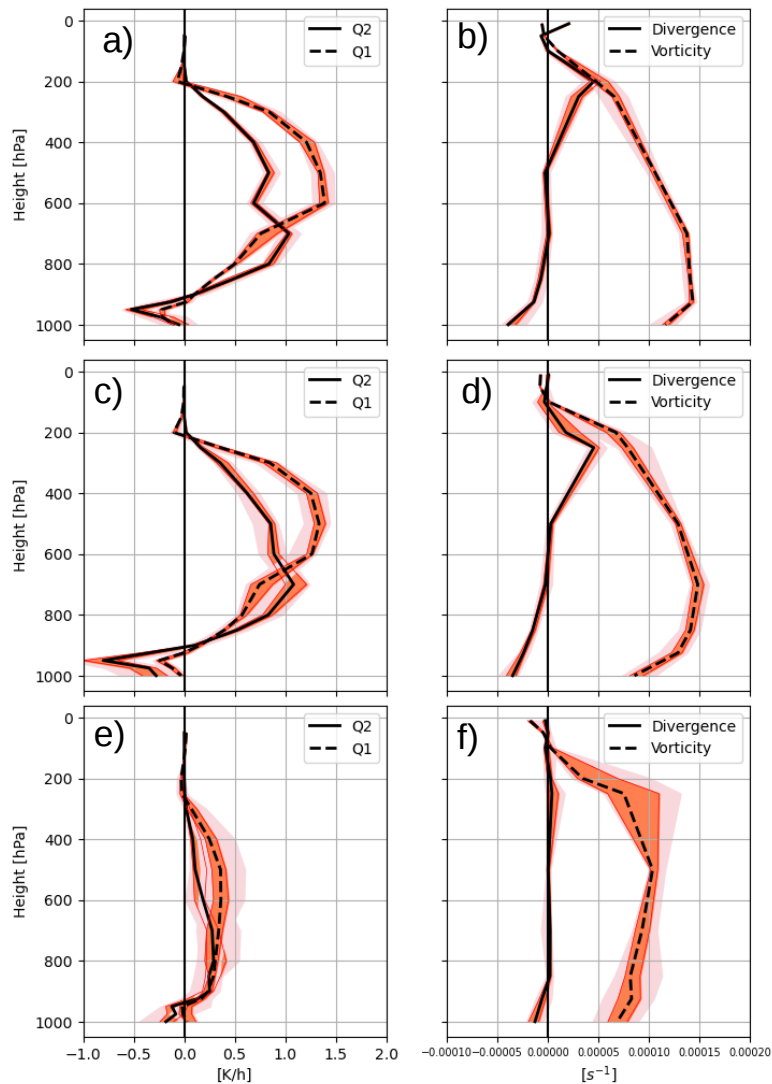
Figure 8. Analysis of the intensification and transition to tropical-like characteristics for Ianos as represented by the SPP-Conv experiment. The $Q1 = \frac{dT}{dt}$ and $Q2 = -\frac{L_v}{c_P}\frac{dq}{dt}$ profiles are shown in the first column and the vorticity and divergence profiles are shown in the second column. Figures (a) and (b) are taken on the 16th of September at 1200 UTC. Figures (c) and (d) are taken on the 17th of September at 0000 UTC. Figures (e) and (f) are taken on the 20th of September at 1200 UTC. These profiles belong to the simulation starting on the 16th.

These results indicate that Ianos and Zorbas are simulated mostly with the right tropical-like phase, with almost the right

460 timing, while the ensemble simulation for Trixie fails to reproduce the right intensification of the cyclone, simulating a shallow warm core on the 28th and missing the deepening on the 30th.
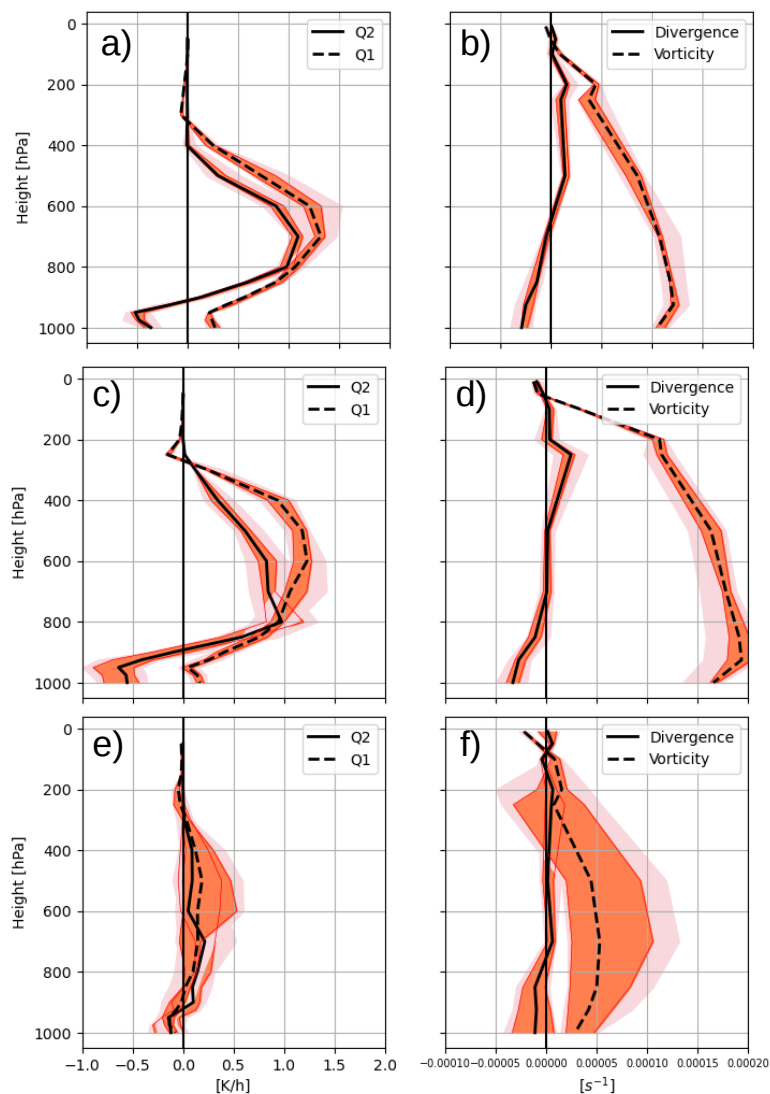
Figure 9. Same as Figure 8 but for Zorbas. Figures (a) and (b) are taken on the 27th of September at 1200 UTC. Figures (c) and (d) are taken on the 28th of September at 1200 UTC. Figures (e) and (f) are taken on the 1st of october at 1200 UTC. These profiles belong to the simulation starting on the 27th.

5   Process behind the intensification of the cyclone

To understand the obtained results concerning the tropical-like phase and the development of the three cyclones, the focus is put on the simulation of the precursor events leading up to the medicanes formation and on the simulation and role played by
465   convective instability and surface forcing for these cyclones.
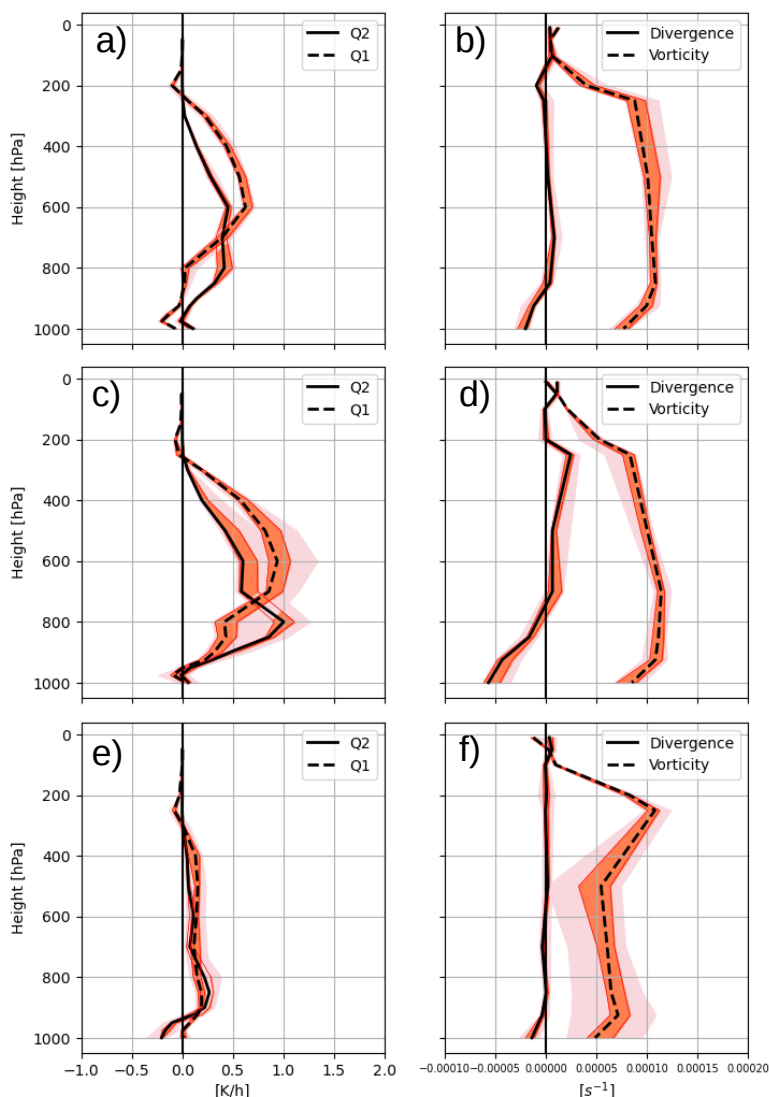
Figure 10. Same as Figure 8 but for Trixie. Figures (a) and (b) are taken on the 27th of October at 1200 UTC. Figures (c) and (d) are taken on the 28th of October at 0000 UTC. Figures (e) and (f) are taken on the 30th of October at 1200 UTC. These profiles belong to the simulation starting on the 27th.

5.1 Dynamical forcing and Potential Vorticity analysis

A crucial factor for the formation of intense Mediterranean cyclones is the presence of air masses with high potential vorticity (PV) to intrude in the Mediterranean region (Flaounas et al., 2022), which usually triggers instability also in the case of extratropical cyclones (Flaounas et al., 2015; Raveh-Rubin and Flaounas, 2017). This stratospheric air mass is able to intro-

470   duce anomalous high PV in the upper troposphere, which induces thermodynamic instability strengthening the surface vortex
below. Usually, this stratospheric air mass intrusion is called PV streamer (Claud et al., 2010) and it is present in all three
medicanes. This is underlined in Figure 11 for the operational analysis in which the height of the isosurfaces of 2 PVU (PVU
$= m^2 K kg^{-1} s^{-1} 10^{-6}$) is shown in relation to the mean sea level pressure for the three medicanes. When the PV anomaly
can detach from the streamer then it continues to sustain the medicane in the tropical-like phase. This is what happens in the
475   case of Ianos (Figure 11a) and Zorbas (not shown for the analysis but reported in Supplementary Figure S6 for the ensemble
experiments).

The detachment from the large-scale hasn't happened yet in Figure 12, but it will happen 12 hours later (Supplementary
Figure S6) which is in line with what is shown in Figure 4 regarding the simulated minimum central pressure reaching the
480   lowest value with a delay compared to the analysis. Nonetheless for Ianos, if starting from the 17th, the three ensembles are
capable of reproducing the PV cut-off from the large scale at the right timing. The PV streamer is well reproduced, especially
regarding its interaction with the Q1 heating at 500 hPa (colored lines in Figure 12a).
For Zorbas, the PV streamer is evident and it is occurring one day prior to the tropical phase (Figure 11b) thus inducing an
intensification of the cyclone. This is well reproduced by the SPP-Conv ensemble experiment shown in Figure 12b, as well as
485   for the other two ensemble simulations INI and SPP. The values of the height of the 2 PVU isosurfaces coincide between the
operational analysis and the ensemble simulations.
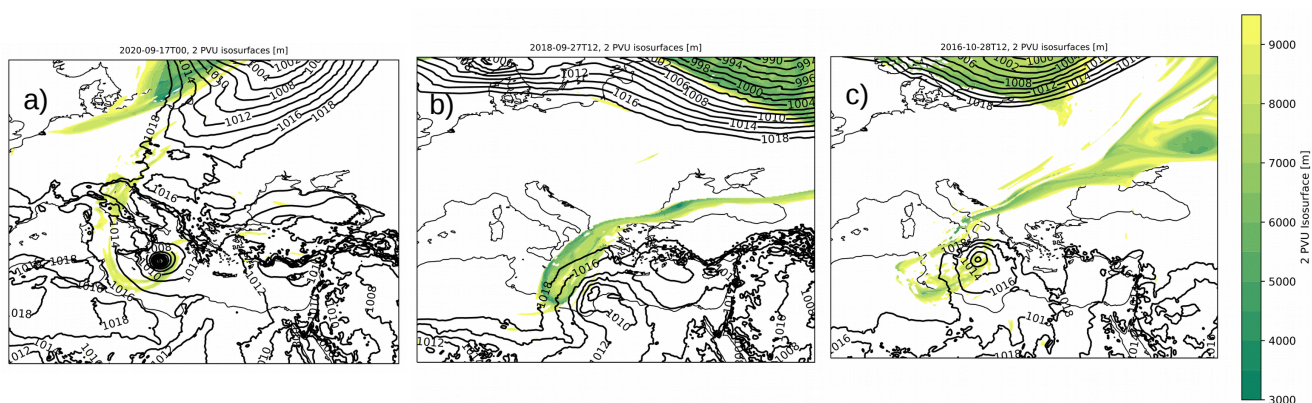
Figure 11. Height of the 2 PVU (PVU = $m^2 K kg^{-1} s^{-1} 10^{-6}$) isosurfaces together with the mean sea level pressure (black lines) in the
operational analysis. For Ianos the 17th at 00 UTC is reported in Figure (a), for Zorbas the 27th at 12 UTC is reported in Figure (b) and for
Trixie the 28th at 12 UTC is reported in Figure (c).

Regarding Trixie, the interaction between the PV streamer and the cyclone is not so evident (Figure 11c), but is reaching the
area in which the cyclone is forming. Moreover, the heating, reported in Figure 12c, is not aligned with the PV streamer. This

490 happens in the timestep where the cyclone is intensifying before dying out in the ensemble simulations (the 28th). In Figure
12c the ensemble mean regarding the simulation starting from the 26th is shown, while for the ensemble mean of the other
starting dates, the 25th in specific, the PV streamer and the surface vortex are further misaligned. Indeed, with the forecast
start date closer to occurrence the alignment is better reproduced (see Supplementary Figure S6). This has played a role in the
missing intensification and tropical phase of the cyclones.

495
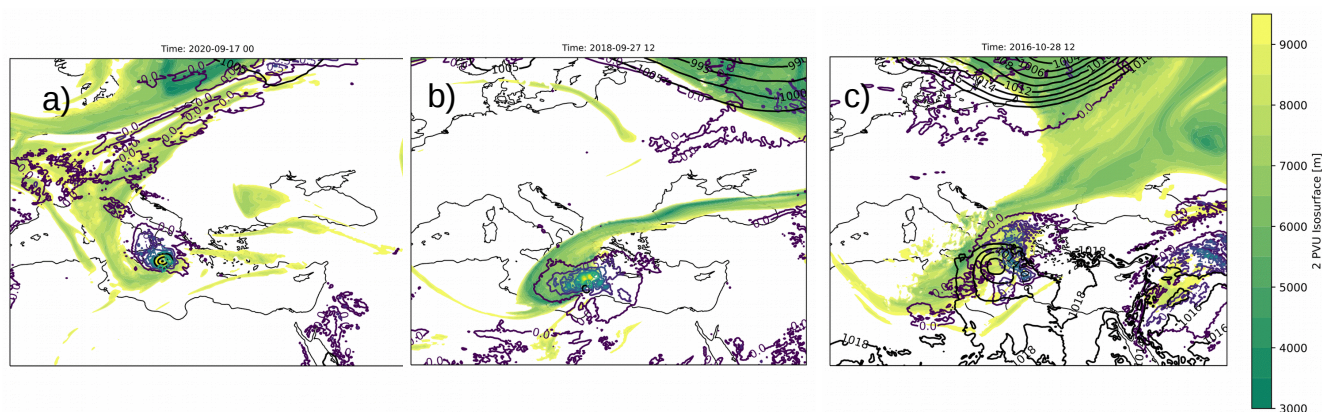
Figure 12. Height of the 2 PVU (PVU = $m^2 K k g^{-1} s^{-1} 10^{-6}$) isosurfaces together with the mean sea level pressure (black lines) and Q1 at
500 hPa for the SPP-Conv ensemble experiment ensemble mean. For Ianos the 17th at 00 UTC is reported in Figure (a) as simulated by the
experiment starting from the 17th, for Zorbas the 27th at 12 UTC is reported in Figure (b) as simulated by the experiment starting from the
26th and for Trixie the 28th at 12 UTC is reported in Figure (c) as simulated by the experiment starting from the 26th.

Indeed, a factor that contributes to the evolution and intensification to reach a tropical-like state is the pairing of the upper-
level instability with the lower-level one. Carrió et al. (2017) underlined the importance of the upper-level dynamics in in-
tensifying the surface vortex and supporting the tropical transition of the cyclone. This is what is shown in Figure 13, which
represents the potential vorticity field and the meridional and zonal winds in a cross-section of latitude and pressure, at differ-
500 ent stages for each medicane for the operational analysis. There, in Figure 13a, d, and g, is present an anomaly of potential
vorticity in the lower troposphere, around 800 hPa, which is a signal of the formation of a surface vortex for all the cyclones
accompanied by a production of PV by diabatic processes. This is happening in the surrounding of the cyclone position. There,
the PV field is shown for the 24 hours before the cyclone became tropical-like. In the upper troposphere, an anomaly of PV is
developing and intruding from the stratosphere. After 12 hours (Figure 13b, e, and h) the two anomalies of PV, the upper-level
505 and the lower-level, start to align. The same mechanism has been recognized in the literature by Cioni et al. (2018); Miglietta
et al. (2017). Finally, the tropical phase is reached when a cyclonic wind circulation completely wraps around the PV anomaly
(Figure 13c f and i).
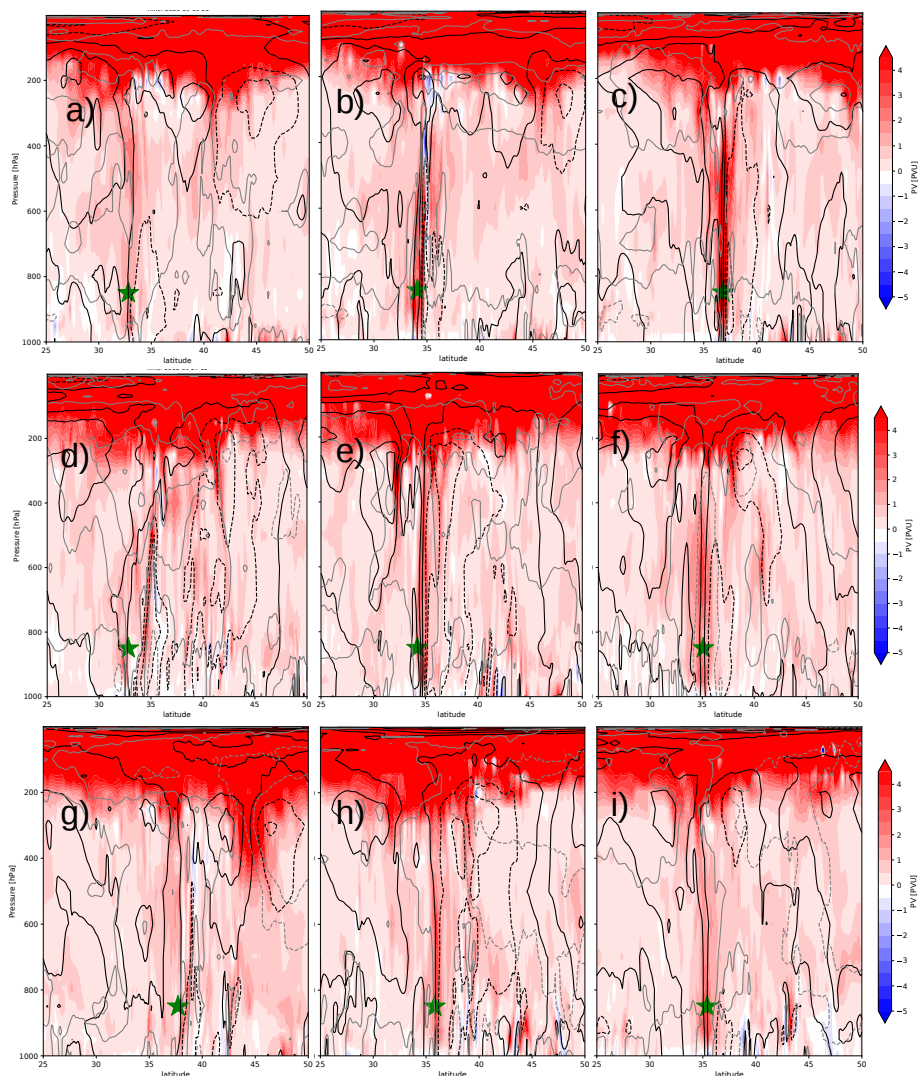
Figure 13. Operational analysis Potential vorticity field cross-section in latitude from 25° to 50° and pressure taken in the longitude of the central minimum pressure of the cyclones (green star). The PV is in colour and the black lines represent the zonal wind, while the gray lines represent the meridional wind. For Ianos the cross sections shown regard the 16th at 00 UTC, the 16 at 12 UTC and the 17th at 00 UTC in Figures (a), (b) and (c) respectively. For Zorbas the cross sections belong to the 27h at 12 UTC, the 28th at 00 UTC and the 28th at 12 UTC in Figures (d), (e) and (f) respectively. For Trixie the cross sections belong to the 29h at 00 UTC, the 29th at 12 UTC and the 30th at 00 UTC in Figures (g), (h) and (i) respectively.

In the simulation of these cyclones, the ensemble experiments behave similarly. For Ianos, the tropical-like phase on the
510 17th of September (Figure 14a and b) is reproduced quite nicely, with the INI experiment presenting slightly weaker PV than

the SPP-Conv ensemble mean (for the simulation starting from the 16th shown in the Figure). For Zorbas, on the 28th, the PV values in the two ensemble experiments are higher than the analysis, signaling a slightly more symmetrical and intense cyclone (Figure 14c and d). However, the two experiment ensemble mean is very similar.

Trixie instead, as mentioned above, does not present enough strong surface vortex to align with the PV anomaly in the upper
515   level for both experiments (Figure 14e and f) for the 25th as the starting date. If one looks into the other starting dates simulation it appears that there is a stronger lower-level instability (not shown).

Thus, the occurrence of a strong surface-level vortex is prevented in the Trixie simulations (Figure 14). This is firstly due to the fact that the alignment of the surface vortex PV production and the upper-level PV is not well reproduced. Furthermore,
520   it has to be pointed out that in the ensemble simulations, there is the absence of a strong cut-off low (deep upper tropospheric trough, cut off from the large-scale circulation), a precursor event that sustains the medicane Emanuel (2005) (Supplementary Figure S5 shows the different reproduction of the cut-off low presence and how it changes with different starting dates). The cut-off low position and intensity have had an influence on the tracking and intensity of Trixie, in accordance with what was suggested in the literature Emanuel (2005). Indeed, in the analysis, there are two distinct lows that form (supplementary Figure
525   S3), and the first one is responsible for the Trixie surface vortex, by bringing instability from the upper troposphere to the lower troposphere. Instead, in the ensemble simulations the formation of the second cut-off low prevails and the first one is weakened (Supplementary Figure S4). With the weakening of the cut-off low, Trixie starts lowering its intensity (around the 29th). Only a few members are able to follow the weak cut-off low (Supplementary Figure S3). This has had an impact on the simulation of the already weak cyclone that is Trixie. Indeed, Trixie is in general weaker than the other two cyclones (the
530   central minimum pressure of Trixie is higher than the other two cyclones, as reported in Table 2), thus there is a chance that this fact has influenced the ensemble simulations. To investigate these aspects the focus is put on some other elements involved in the development of Trixie.

5.2   Convective Instability and surface forcing

535   First of all, the Convective Available Potential Energy (CAPE) has been analyzed for the three medicanes and specifically for Trixie, showing weaker convection indicated by a weaker CAPE. Indeed in Figure 15 there is a comparison between CAPE around the cyclone centre for Zorbas and Trixie at the intensification tropical-like state. The reduced convective activity reported in Figure 15 for Trixie underlines the lower energy production due to diabatic heating in Trixie ensembles simulations. Such a situation can be ineffective to drive the cyclone to a state in which it is able self-sustain by the wind-induced surface
540   fluxes (Emanuel, 1986) and the transition to the tropical-like cyclone being degraded as already found in Koseki et al. (2021). This is correlated with the surface fluxes, being much higher in the case of Zorbas and Ianos compared to Trixie (Supplementary Figure S7). By the 29th of October, in the Trixie simulation, the convection is weakening and by the 30th is absent in the ensemble experiments, compared to the analysis. Thus this reduced CAPE in the ensemble simulations is signaling a simulated
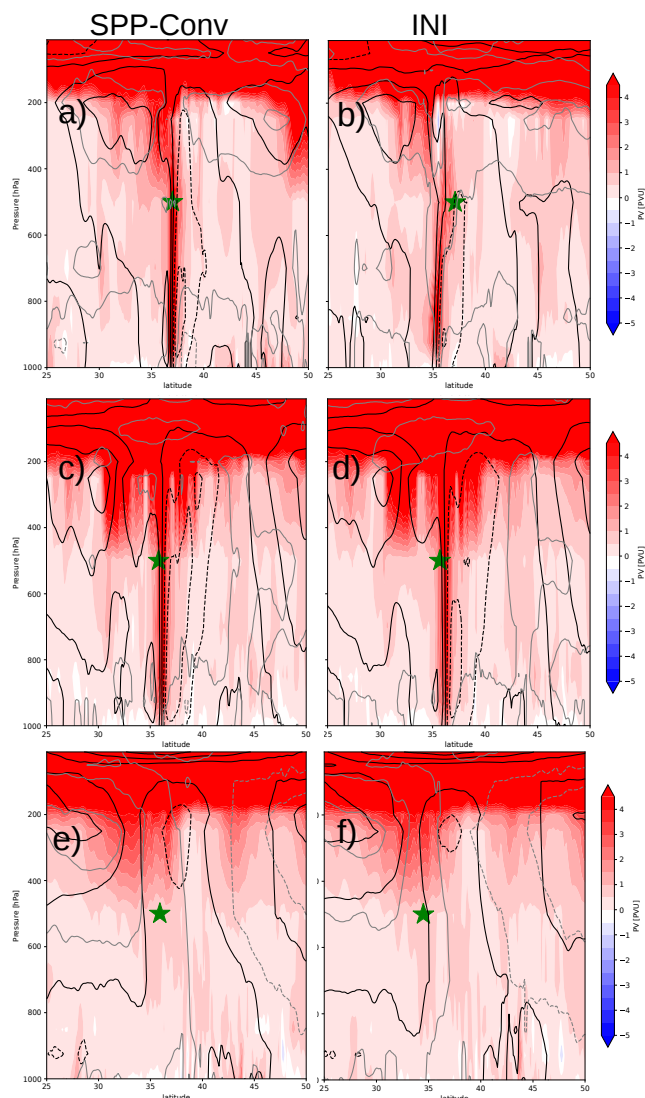
Figure 14. Potential vorticity field cross-section in latitude from 25° to 50° and pressure taken in the longitude of the central minimum pressure of the cyclones (green star) as represented by the SPP-Conv and the INI ensemble means in the first and second column respectively. The PV is in colour and the black lines represent the zonal wind, while the gray lines represent the meridional wind. For Ianos the cross sections shown regard the 17th at 00 UTC in Figures (a) and (b). For Zorbas the cross sections belong to the 28th at 12 UTC in Figures (c) and (d). For Trixie the 30th at 00 UTC is shown in Figures (e) and (f) respectively.

weaker low-level vortex.

545
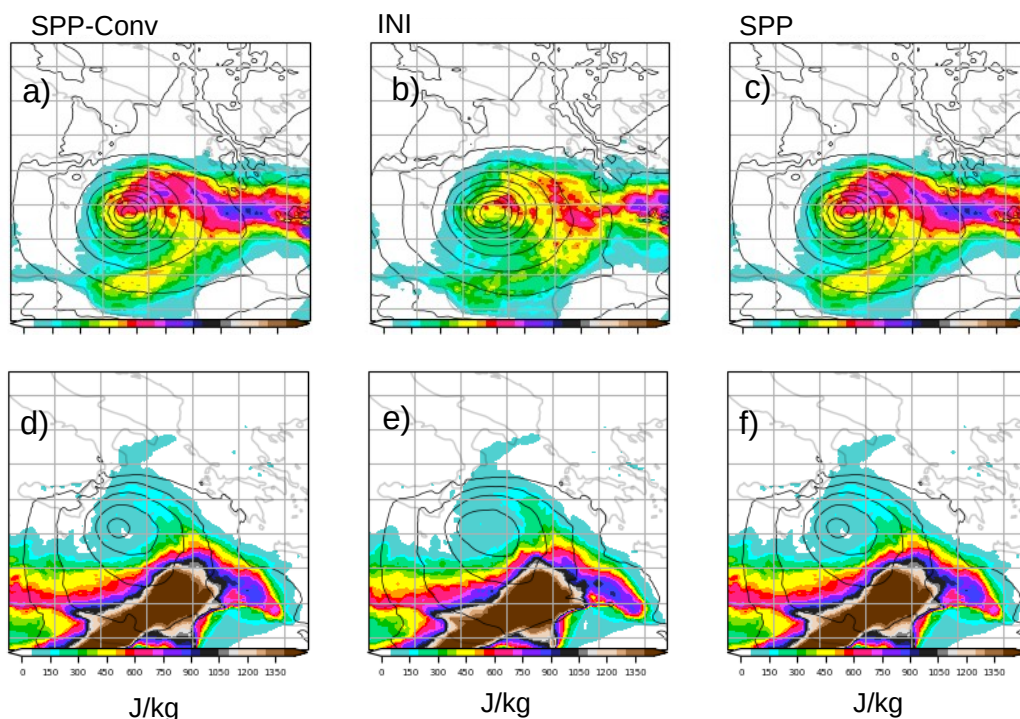
Figure 15. Convective Available Potential Energy (J/kg) (in colours) and mean sea level pressure (in lines) for the three ensemble experiments ensemble means. For Zorbas the 28th at 12 UTC is shown in Figures (a), (b) and (c) for the simulation starting from the 27th. For Trixie the 28th at 12 UTC is shown in Figures (d) (e) and (f) for the simulation starting from the 27th.

By looking at the Sea Surface Temperature (SST) anomaly, it is found that it is higher for Zorbas (Ianos is once again similarly affected by the SST anomaly as Zorbas) upon formation compared to Trixie, as reported in Figure 16 which is showing the ensemble mean anomaly of the SPP-Conv and INI experiments for Zorbas and Trixie for comparison. There, it is shown that if on one hand, for Zorbas (Figure 16a b and c) the SST is anomalously high compared to the climatological SST of September
550 (obtained by using the ERA5 reanalysis SSTs over the Mediterranean Basin from 1991 to 2020), of on average 2°, for Trixie the anomaly (with respect to the climatological SST of October) decreases, and in the area of cyclone formation is very weak compared to Zorbas (Figure 16d, e and f). This means that the air-sea temperature contrast did not play a crucial role in Trixie generation and maintenance as it did for Ianos and Zorbas, probably resulting in weaker low-level vortex altogether.

555   Indeed, the ensemble experiments results compare fairly well to the operational analysis for the SST anomaly for the three medicanes (not shown), underlining the relative importance of the air-sea interaction in the tropicalization of the Mediterranean cyclones. The higher surface temperatures in Ianos and Zorbas help feed the medicane the moisture, through surface fluxes (Pytharoulis, 2018), allowing the convection to develop more effectively (Koseki et al., 2021; Cioni et al., 2018). Thus, it is
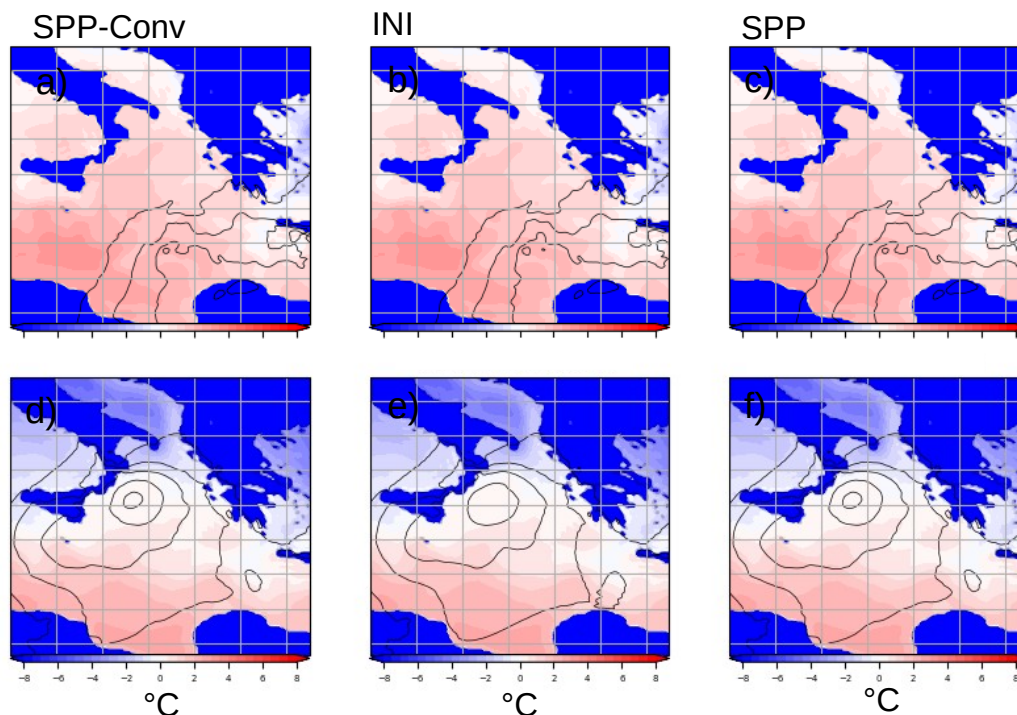
Figure 16. Sea surface Temperature anomaly (°C) (in colours) and mean sea level pressure (in lines) for the three ensemble experiments ensemble means. For Zorbas the 27th at 00 UTC is shown in Figures (a), (b) and (c) for the simulation starting from the 27th. For Trixie the 28th at 00 UTC is shown in Figures (d) (e) and (f) for the simulation starting from the 27th.

evinced that Zorbas and Ianos tropical-like phase is also sustained by diabatic processes, while Trixie is not.

560

Indeed, it is hypothesized that Trixie is formed as a lower-level vortex mainly due to the thermodynamic disequilibrium generated by the upper-level cut-off low. Thus, if the latter is not well simulated, being weaker, it is not able to sustain the surface vortex. In turn, the surface level production of PV is not enough to match with the upper tropospheric high PV field as in Figure 14e and f. There, the convective-generated PV is not strong enough or not able to align with the upper-level one.

565 Indeed, the interaction between the two latter, the convectively produced PV at low levels, and the PV streamer aloft has been deemed to be crucial for the development of the Mediterranean cyclones (Cioni et al., 2018).

The intensification of the cyclone is better captured by increasing the starting date (as it is shown in Supplementary Figure S6), because with forecast start date closer to occurrence the alignment is better reproduced and also there is more low-level

570 PV production. However, the cyclone still dies before the 30th of October, due to the low-level vortex being too weak that is not able to interact properly with the upper-level disturbances. Indeed in the operational analysis, it is evident that after the 29th the upper tropospheric perturbation is cut off from the large scale, resembling what is happening in the case of Ianos and Zorbas

(Figure 12b), while this is isn't the case in the ensemble experiments. There the surface vortex disappears with the weakening of the upper-level cut-off low, and due to the absence of a reinforcement of the lower level PV production by the upper level one.

575

Homar et al. (2003) showed that the upper-level PV structure indirectly acts on the cyclone deepening through a modification of the surface circulation. Thus, it is very likely that the modification of PV in the simulations affects the forecast of the trajectory and of the intensity, when the alignment of the upper-level PV and of the lower-level one is absent. Furthermore, a fact that seems to be important in all three cyclones is the simulation of strong convective activity, which is associated with

580 latent heat release, developing in the central region of the cyclones (Figure 8, 9 and 10). Indeed is deep moist convection that is the main mechanism leading to the maintenance and deepening of the system (Cioni et al., 2016, 2018; Flaounas et al., 2022), and its weakening or even absence compromises the forecast. The simulation intensification phase and timing are probably dependent on how the convection is reproduced. In Trixie, the starting dates are probably too early to reproduce the right convective activity to sustain the cyclone.

585

To conclude, the right positioning of the PV streamer in the intensification of these types of Mediterranean cyclones had been recognized by Portmann et al. (2020). There they applied it to one of the medicanes here studied, Zorbas. In their study, they reported that the correct, PV streamer position resulted in the most accurate forecasts with a strong medicane in most members, up to three days prior to intensification. In this study, this is the right temporal range to observe a good forecast for

590 Zorbas and Ianos, while for Trixie one can clearly see how this uncertainty is affecting the forecast.

6 Discussion

Predicting and simulating medicanes is a difficult task due to them being extreme events found near the tail of the forecast distribution (Majumdar and Torn, 2014) and due to the complexity of the processes involved. The specific barriers to predictability and the atmospheric conditions that lead to medicanes formation and evolution are not fully understood. Research

595 utilizing multi-physics approaches has found that the track, intensity, and duration of medicanes are heavily sensitive to factors such as convection, microphysics, and boundary-layer parameterizations (Ragone et al., 2018; Miglietta et al., 2015). This study indeed is a first step towards the understanding of this sensitivity by using ensemble forecast simulation.

The analysis has been focused on three medicanes with the use of the ECMWF model IFS ensemble forecast system. Three

600 experiments were conducted, the operational ensemble forecast with the perturbation at initial conditions, INI, two experiments with SPP, in one case perturbing only the parameters of the convection parameterization, SPP-Conv, and in the other perturbing the parameters of all relevant physical parameterizations, SPP. The used approach has been aimed at the analysis first and foremost of tracking and intensity, meaning central pressure. Secondly, the precipitation field has been analyzed, and finally, the focus has been put on the parameters characterizing the thermal structure of the cyclone and its asymmetry, the convective

605   heating and the development processes.

From the study, it was found that the use of SPP, and specifically the perturbation of convective parameters (SPP-Conv), in terms of tracking spread and precipitation intensity compare well to the INI experiment. Similar results have been obtained also in Ollinaho et al. (2017b), especially regarding precipitation. The three experiments are usually under dispersive when it

610   comes to tracking position, even if the INI experiment is giving better results. It has to be noted that the ensemble spread and mean are usually lower in the SPP experiments. Nonetheless the latter are able to produce the same spread as the initial condition perturbation experiment, underlying the benefit of the introduction of perturbations of physical parameters, especially regarding convection, in comparison with only using the perturbations of the initial conditions (Lang et al., 2012; Ollinaho et al., 2017b).

615

Regarding the reproduction of the minimum central pressure by the ensemble forecasts (Figure 4) it is found that in general there is a time shift in the reproduction of the minimum intensity, where both Ianos and Zorbas ensemble mean reach the maximum intensity with a delay. Since the delay is decreasing with forecast start date closer to occurrence, this is attributable to improved initial conditions. Regarding Ianos and Zorbas, the ensemble spread for the SPP experiments is able to include the

620   analysis one, similarly to the INI experiment (Figure 4).

By looking at the simulated precipitation distribution, compared to the GPM-IMERG satellite observations, show that only for Ianos, the precipitation field is well reproduced by the ensembles, with the INI experiment being slightly more intense than the SPP and SPP-Conv experiments. Even if the GPM-IMERG dataset, tends to overestimate precipitation over the Mediter-

625   ranean, the precipitation simulated for Zorbas and Trixie is too weak. However, it is discussed that in general, the precipitation maximum compares better with forecast start date closer to occurrence, thus for Zorbas, starting the ensemble forecasts on the 28th would have shown better-simulated precipitation. However, the precipitation maximum values are slightly better simulated by the INI experiment also for Zorbas. The analysis of the precipitation field deepened by computing some statistical scores and the results show that the SPP-Conv is slightly better than the SPP and INI experiment. The BS score results are quite

630   similar between the three experiments and generally show how the three ensemble forecasts perform better than the control forecast. Furthermore, all three forecasts present useful values in terms of precipitation prediction (Buizza et al., 2008), being higher than 0.5 and in most cases higher than 0.7. The most significant values, occur in Ianos, making it the most well-captured storm of the three.

635   Regarding the tracking, the precipitation and the intensity of the cyclone there is a common gradual decrease of the error with forecast start date closer to occurrence. This is consistent for all three ensemble experiments and it is specific for Ianos and Zorbas. Usually, the later starting forecasts tend to be more accurate (lower error and spread). For Trixie this decrease in the error is weaker and in some cases nonexistent. Indeed, as pointed out in the results the simulation of this particular cyclone

can be considered a missed forecast.

640

Through tracking, it was verified that with regard to the Trixie simulation, there is a southeastward shift of the trajectory with respect to the analysis and, that, among the three storms, the best predicted is Ianos. The southeastward shift was identified after the analysis of the ensemble spread and error. A lower spread in the tracked position was found for Zorbas and Ianos compared to Trixie, but the error of Trixie exceeds 800 km. This is attributable to the fact that the ensemble forecast starts too

645 early with respect to the cyclone intensification phase for Trixie. This result, in particular, aligns with previous studies that had pointed to Trixie's low occurrence probability up to two days earlier (Di Muzio et al., 2019). Indeed, There is an inherently low probability of medicanes occurrence (as seen in Di Muzio et al. (2019)) and the development of a warm core cyclone depends on many factors, large-scale factors and small-scale factors like surface fluxes, that can be improved by the initial conditions of a preexisting cyclone. The decrease of the spread at later starting dates in Trixie can be correlated with the higher probability

650 of occurrence and the better reproduction of the physical processes leading to cyclone intensification.

Indeed, the factors that have played a role in the forecasts missing the tracking position and intensification have been found to be linked to the simulations of the development processes. Besides the missing intensification of the precursor cut-off low, the factor that has been recognized to be of primary importance in the development of these types of Mediterranean cyclones

655 is the simulation of the alignment between the upper-level and the lower-level regions with high values of PV (Carrió et al., 2017; Cioni et al., 2018; Flaounas et al., 2022). This happens specifically for Trixie, but it is also true for Ianos and Zorbas, especially with the timing shift with which they intensify.

By the analysis of the cyclone thermal structure and symmetry and the Q1 and Q2 profiles, it is shown that if for Ianos and

660 Zorbas the tropical-like phase is reached, with a gradual evolution of the error and spread, where there is a lowering of the spread accompanied by the distribution approaching the reference values (upper-level thermal wind in Figure ?? and ??). In those cases, the forecasts are accurate at reproducing both the thermal structure and symmetry of the cyclones, compared to the analysis value. Both Zorbas and Ianos deep warm core phase is well captured, especially with forecast start date closer to occurrence.

665 The only exception to the reasonable reproduction of the storm thermal structure is the upper-level thermal wind in Trixie (Figures ??a-c-e). This means that for Trixie, where the analysis value reported the presence of a warm core ($-V_T^U = 25$ in Table 2), the three ensemble forecast presents a cold core cyclone (negative $-V_T^U$ values). This, together with the underestimation of the deepening of the cyclone, can explain the low scores for the precipitation analysis since the simulated cyclone is not able to reach the warm core, thus the convective heating is lower affecting the simulation of the precipitation. From the Q1 and

670 Q2 profiles, it is evinced that the cyclone seems to intensify around the 28th and to die out by the 30th, when it was actually supposed to enter the tropical-like phase. Also in Dafis et al. (2020) it was reported that a second intensification occurred in Trixie around the 30th due to deep convection activity.

In general, the analysis of the thermal structure and symmetry indicates that for the upper-level thermal wind, the smaller spread is in most cases obtained in the SPP-Conv experiment (in particular at later forecasts), while the spread is comparable for the three ensemble experiments regarding the thermal symmetry. This once again points out the possibility of using SPP in ensemble forecasting to generate a similar spread in the ensemble distributions compared to only using initial conditions perturbations. Indeed the ensemble experiments behave similarly regarding the simulation of the tropical-like characteristics of the three cyclones. Furthermore, the SPP and SPP-Conv experiments are found to be extremely similar, possibly meaning that the uncertainties linked to the convection parameterization are predominant in the simulation of these types of phenomena.

To answer the question of why Trixie has not been well simulated in comparison with the other two medicanes presented in the study, the analysis of the synoptic situation and physical process involved in the genesis and maintenance of the medicanes has been carried out. From the analysis of the 2 PV isosurfaces and the PV field cross-section revealed that the interaction between the upper-level stratospheric PV intruding in the upper troposphere and the lower-level PV generated by convective heating is key for the intensification and maintenance of Trixie. The later the starting date the greater the misalignment (or the worse positioning of the upper-level disturbance) between the lower and the upper PV production. As mentioned earlier, this is in line with what was found in the literature. Indeed, in many studies, also using the ECMWF ensemble forecasting system (Portmann et al., 2020; Chaboureau et al., 2012), it was found that later forecasts are able to capture better the thermal structure of the medicanes, due to the lower uncertainty of the positioning of PV streamer connected to the generation of the medicane. This is true not only in the case of Trixie but also in Zorbas and Ianos, where the error and the spread are lowered for the ensemble forecasts due to the better reproduction of these features.

However, in the case of Trixie, it also has to be noticed that the fact that it is a weaker medicane compared to Ianos and Zorbas influences the simulations. Indeed, it has been shown that the surface fluxes in the phase of tropicalization and intensification are lower than the other medicanes and the cyclone tends to shut off when the cut-off low vanishes and generally tend to follow the PV streamer. This makes it more subject to being more dependent on the simulation of large-scale processes and more prone to being simulated more weakly than the other two. The three medicanes seem to belong to different medicanes categories of the medicane classification (Miglietta and Rotunno, 2019; Dafis et al., 2020; Flaounas et al., 2022). Specifically, in Miglietta and Rotunno (2019) and Flaounas et al. (2022) three distinct categories of medicanes are distinguished: one in which baroclinic instability plays an important role throughout the cyclone's lifetime and most of their intensification is due to convection (Fita and Flaounas, 2018); and one in which baroclinicity is important only in the initial stage and, the theory of wind-induced surface heat exchange (WISHE (Emanuel, 1986)) is behind their intensification through positive feedback between the latent heat release and the air-sea interactions and one in which there is a synergy between baroclinic and diabatic processes (and control from the SST over the cyclone (Pytharoulis et al., 2000)). The first type is possibly Trixie's family and Ianos and Zorbas belong to the second and third types respectively. Thus in this study, it is found that the ensemble forecasting of ECMWF is able to better capture the tropical-like features of the second and third categories o medicanes. The investigation of this will be the subject of further study, also considering a greater number of medicanes.

7   Conclusions

710 To sum up, by considering all the parameters used in this analysis, it can be assessed that the ECMWF ensemble forecasts model can adequately reproduce medicanes with their tropical-like features, given a correct representation of the large-scale circulation. The result of this study, compared to previous ones (Di Muzio et al., 2019; Chaboureau et al., 2012; Pantillon et al., 2013), which used only the operation ensemble forecast of ECMWF, points out the benefit of using the Stochastically Perturbed Parameterization, SPP ensemble forecast compared to only perturbing the initial conditions. The SPP, especially the

715 SPP-Conv experiments, show in some cases lower but comparable spread and spread-skill score values and better precipitation scores than the INI experiment.

Regarding the physical processes linked to the ensemble forecasting results, this study confirms that similar processes are at play in the development of the Mediterranean tropical-like cyclones and the predictability of these cyclones is linked to not only

720 the reproduction of the precursor events (namely the deep cut-off low) but also to the interaction of the upper-level dynamics with the lower-level one (namely the PV streamer and the lower level PV production), in a similar way. This work, as urged in the literature (Dafis et al., 2020; Pytharoulis, 2018) underlines the relative importance of the upper-tropospheric troughs and PV streamer interactions with the troposphere for medicanes not only in one specific case, as often done in the literature (Portmann et al., 2020; Chaboureau et al., 2012; Cioni et al., 2018), but extending the analysis at least to a few different cases.

725

Finally, as discussed in Flaounas et al. (2022) the representation of cloud adiabatic processes is often believed to be a source of forecast uncertainty but dominated by the one created by initial conditions. This study, by comparing ensemble forecasts with the account of initial condition perturbation only and of physical parameterization only, underlines that the uncertainty produced by both ensembles is actually similar. This is due to the found similar spread/skill relationship for the tracking and

730 similar scores for what concerns the intensity of precipitation and the reproduction of the cyclone intensity.

Code and data availability.   The output of the IFS ensemble forecasts and the operational analysis data are available on the MARS Archive at https://www.ecmwf.int/en/forecasts/dataset/ecmwf-research-experiments and the precipitation dataset GPM-IMERG used for validation is freely available on the NASA data archives at https://gpm.nasa.gov/data/imerg. The python codes used to produce the analysis are available at https://doi.org/10.5281/zenodo.7912957.

735 *Author contributions.*   All authors contributed to the conceptualization of the research. P.B., M.S., and P.B.C. worked on the methodology. P.B. carried out the ensemble simulations. M.S. and L.S. carried out the analysis of the ensemble simulations and P.B.C. supervised all the research group work. M.S. and P.B. wrote the original draft. All authors have read, reviewed, edited, and agreed to the manuscript.

Competing interests. No competing interests are present

Acknowledgements. This research has been funded by the Italian Ministry of University and Research (MIUR) and the University of Pe-
740 rugia within the program *Dipartimenti di Eccellenza 2018-2022*, by the *Fondo Ricerca di Ateneo esercizio 2021: Cambiamenti climatici:
consapevolezza impatto sociale, modelli scientifici e soluzioni tecnologiche* and by the European Centre of Medium Range Weather Forecast
(ECMWF). The authors are grateful to Simon Lang and Martin Leutbecher for developing and providing the experimental SPP configuration
and want to acknowledge high-performance computing support from ECMWF Supercomputing HPC facilities.

References

745 Baker, L., Rudd, A., Migliorini, S., and Bannister, R.: Representation of model error in a convective-scale ensemble prediction system, Nonlinear Processes in Geophysics, 21, 19–39, 2014.

Bechtold, P., Köhler, M., Jung, T., Doblas-Reyes, F., Leutbecher, M., Rodwell, M. J., Vitart, F., and Balsamo, G.: Advances in simulating atmospheric variability with the ECMWF model: From synoptic to decadal time-scales, Quarterly Journal of the Royal Meteorological Society: A journal of the atmospheric sciences, applied meteorology and physical oceanography, 134, 1337–1351, 2008.

750 Beljaars, A. C., Brown, A. R., and Wood, N.: A new parametrization of turbulent orographic form drag, Quarterly Journal of the Royal Meteorological Society, 130, 1327–1347, 2004.

Brier, G. W. et al.: Verification of forecasts expressed in terms of probability, Monthly weather review, 78, 1–3, 1950.

Buizza, R.: The value of probabilistic prediction, Atmospheric Science Letters, 9, 36–42, 2008.

Buizza, R. and Hollingsworth, A.: Storm prediction over Europe using the ECMWF ensemble prediction system, Meteorological Applica-
755 tions, 9, 289–305, 2002.

Buizza, R., Milleer, M., and Palmer, T. N.: Stochastic representation of model uncertainties in the ECMWF ensemble prediction system, Quarterly Journal of the Royal Meteorological Society, 125, 2887–2908, 1999.

Buizza, R., Leutbecher, M., and Isaksen, L.: Potential use of an ensemble of analyses in the ECMWF Ensemble Prediction System, Quarterly Journal of the Royal Meteorological Society: A journal of the atmospheric sciences, applied meteorology and physical oceanography, 134,
760 2051–2066, 2008.

Carrió, D., Homar, V., Jansa, A., Romero, R., and Picornell, M.: Tropicalization process of the 7 November 2014 Mediterranean cyclone: Numerical sensitivity study, Atmospheric Research, 197, 300–312, 2017.

Cavicchia, L., von Storch, H., and Gualdi, S.: A long-term climatology of medicanes, Climate dynamics, 43, 1183–1195, 2014.

Chaboureau, J. P., Pantillon, F., Lambert, D., Richard, E., and Claud, C.: Tropical transition of a Mediterranean storm by jet crossing,
765 Quarterly Journal of the Royal Meteorological Society, 138, 596–611, https://doi.org/10.1002/qj.960, 2012.

Christensen, H. M., Moroz, I., and Palmer, T.: Stochastic and perturbed parameter representations of model uncertainty in convection param-eterization, Journal of the Atmospheric Sciences, 72, 2525–2544, 2015.

Cioni, G., Malguzzi, P., and Buzzi, A.: Thermal structure and dynamical precursor of a Mediterranean tropical-like cyclone, Quarterly Journal of the Royal Meteorological Society, 142, 1757–1766, 2016.

770 Cioni, G., Cerrai, D., and Klocke, D.: Investigating the predictability of a Mediterranean tropical-like cyclone using a storm-resolving model, Quarterly Journal of the Royal Meteorological Society, 144, 1598–1610, 2018.

Claud, C., Alhammoud, B., Funatsu, B. M., and Chaboureau, J.-P.: Mediterranean hurricanes: large-scale environment and convective and precipitating areas from satellite microwave observations, Natural Hazards and Earth System Sciences, 10, 2199–2213, 2010.

Comellas Prat, A., Federico, S., Torcasio, R. C., D'Adderio, L. P., Dietrich, S., and Panegrossi, G.: Evaluation of the Sensitivity of Medicane
775 Ianos to Model Microphysics and Initial Conditions Using Satellite Measurements, Remote Sensing, 13, 4984, 2021.

Dafis, S., Claud, C., Kotroni, V., Lagouvardos, K., and Rysman, J.-F.: Insights into the convective evolution of Mediterranean tropical-like cyclones, Quarterly Journal of the Royal Meteorological Society, 146, 4147–4169, 2020.

Davis, C.: Resolving tropical cyclone intensity in models, Geophysical Research Letters, 45, 2082–2087, 2018.

Davolio, S., Miglietta, M., Moscatello, A., Pacifico, F., Buzzi, A., and Rotunno, R.: Numerical forecast and analysis of a tropical-like cyclone
780 in the Ionian Sea, Natural Hazards and Earth System Sciences, 9, 551–562, 2009.

Di Muzio, E., Riemer, M., Fink, A. H., and Maier-Gerber, M.: Assessing the predictability of Medicanes in ECMWF ensemble forecasts using an object-based approach, Quarterly Journal of the Royal Meteorological Society, 145, 1202–1217, 2019.

Emanuel, K.: Genesis and maintenance of" Mediterranean hurricanes", Advances in Geosciences, 2, 217–220, 2005.

Emanuel, K. A.: An air-sea interaction theory for tropical cyclones. Part I: Steady-state maintenance, Journal of Atmospheric Sciences, 43, 585–605, 1986.

Ernst, J. and Matson, M.: A Mediterranean tropical storm?, Weather, 38, 332–337, 1983.

Fita, L. and Flaounas, E.: Medicanes as subtropical cyclones: The December 2005 case from the perspective of surface pressure tendency diagnostics and atmospheric water budget, Quarterly Journal of the Royal Meteorological Society, 144, 1028–1044, 2018.

Flaounas, E., Raveh-Rubin, S., Wernli, H., Drobinski, P., and Bastin, S.: The dynamical structure of intense Mediterranean cyclones, Climate Dynamics, 44, 2411–2427, 2015.

Flaounas, E., Kotroni, V., Lagouvardos, K., Gray, S. L., Rysman, J.-F., and Claud, C.: Heavy rainfall in Mediterranean cyclones. Part I: contribution of deep convection and warm conveyor belt, Climate dynamics, 50, 2935–2949, 2018.

Flaounas, E., Davolio, S., Raveh-Rubin, S., Pantillon, F., Miglietta, M. M., Gaertner, M. A., Hatzaki, M., Homar, V., Khodayar, S., Korres, G., et al.: Mediterranean cyclones: Current knowledge and open questions on dynamics, prediction, climatology and impacts, Weather and Climate Dynamics, 3, 173–208, 2022.

Forbes, R. M., Tompkins, A. M., and Untch, A.: A new prognostic bulk microphysics scheme for the IFS, 2011.

Frogner, I.-L., Andrae, U., Ollinaho, P., Hally, A., Hämäläinen, K., Kauhanen, J., Ivarsson, K.-I., and Yazgi, D.: Model uncertainty representation in a convection-permitting ensemble—SPP and SPPT in HarmonEPS, Monthly Weather Review, 150, 775–795, 2022.

Geetha, B. and Balachandran, S.: Diabatic heating and convective asymmetries during rapid intensity changes of tropical cyclones over North Indian Ocean, Tropical Cyclone Research and Review, 5, 32–46, 2016.

Goosse, H. and Fichefet, T.: Importance of ice-ocean interactions for the global ocean circulation: A model study, Journal of Geophysical Research: Oceans, 104, 23 337–23 355, 1999.

Grabowski, W. W., Wu, X., and Moncrieff, M. W.: Cloud resolving modeling of tropical cloud systems during Phase III of GATE. Part III: Effects of cloud microphysics, Journal of the atmospheric sciences, 56, 2384–2402, 1999.

Hamill, T. M., Whitaker, J. S., Fiorino, M., and Benjamin, S. G.: Global ensemble predictions of 2009's tropical cyclones initialized with an ensemble Kalman filter, Monthly Weather Review, 139, 668–688, 2011.

Hart, R. E.: A cyclone phase space derived from thermal wind and thermal asymmetry, Monthly weather review, 131, 585–616, 2003.

Hart, R. E. and Evans, J. L.: A climatology of the extratropical transition of Atlantic tropical cyclones, Journal of Climate, 14, 546–564, 2001.

Hogan, R. J. and Bozzo, A.: A flexible and efficient radiation scheme for the ECMWF model, Journal of Advances in Modeling Earth Systems, 10, 1990–2008, 2018.

Homar, V., Romero, R., Stensrud, D., Ramis, C., and Alonso, S.: Numerical diagnosis of a small, quasi-tropical cyclone over the western Mediterranean: Dynamical vs. boundary factors, Quarterly Journal of the Royal Meteorological Society: A journal of the atmospheric sciences, applied meteorology and physical oceanography, 129, 1469–1490, 2003.

Huffman, G. J., Bolvin, D. T., Braithwaite, D., Hsu, K.-L., Joyce, R. J., Kidd, C., Nelkin, E. J., Sorooshian, S., Stocker, E. F., Tan, J., et al.: Integrated multi-satellite retrievals for the global precipitation measurement (GPM) mission (IMERG), in: Satellite precipitation measurement, pp. 343–353, Springer, 2020.

IFS Documentation CY47R3, E.: IFS Documentation CY47R3 Part IV Physical processes, 2021a.

IFS Documentation CY47R3, E.: IFS Documentation CY47R3 Part V Ensemble prediction system, 2021b.

820 IFS Documentation CY47R3, E.: IFS Documentation CY47R3 Part VII ECMWF Wave model, 2021c.

Köhler, M., Ahlgrimm, M., and Beljaars, A.: Unified treatment of dry convective and stratocumulus-topped boundary layers in the ECMWF model, Quarterly Journal of the Royal Meteorological Society, 137, 43–57, 2011.

Koseki, S., Mooney, P. A., Cabos, W., Gaertner, M. Á., de la Vara, A., and González-Alemán, J. J.: Modelling a tropical-like cyclone in the Mediterranean Sea under present and warmer climate, Natural Hazards and Earth System Sciences, 21, 53–71, 2021.

825 Lagouvardos, K., Karagiannidis, A., Dafis, S., Kalimeris, A., and Kotroni, V.: Ianos—A hurricane in the Mediterranean, Bulletin of the American Meteorological Society, 103, E1621–E1636, 2022.

Lang, S., Leutbecher, M., and Jones, S.: Impact of perturbation methods in the ECMWF ensemble prediction system on tropical cyclone forecasts, Quarterly Journal of the Royal Meteorological Society, 138, 2030–2046, 2012.

Lang, S. T., Lock, S.-J., Leutbecher, M., Bechtold, P., and Forbes, R. M.: Revision of the stochastically perturbed parametrisations model

830 uncertainty scheme in the integrated forecasting system, Quarterly Journal of the Royal Meteorological Society, 147, 1364–1381, 2021.

Lin, J. and Qian, T.: Rapid intensification of tropical cyclones observed by AMSU satellites, Geophysical Research Letters, 46, 7054–7062, 2019.

Magnusson, L., Thorpe, A., Buizza, R., Rabier, F., and Nicolau, J.: Predicting this year's European heat wave, ECMWF Newsletter, 145, 4–5, 2015.

835 Majumdar, S. J. and Torn, R. D.: Probabilistic verification of global and mesoscale ensemble forecasts of tropical cyclogenesis, Weather and Forecasting, 29, 1181–1198, 2014.

Malardel, S., Wedi, N., Deconinck, W., Diamantakis, M., Kühnlein, C., Mozdzynski, G., Hamrud, M., and Smolarkiewicz, P.: A new grid for the IFS, ECMWF newsletter, 146, 321, 2016.

Marsigli, C., Montani, A., and Paccangnella, T.: A spatial verification method applied to the evaluation of high-resolution ensemble forecasts,

840 Meteorological Applications: A journal of forecasting, practical applications, training techniques and modelling, 15, 125–143, 2008.

Mazza, E., Ulbrich, U., and Klein, R.: The tropical transition of the October 1996 medicane in the western Mediterranean Sea: A warm seclusion event, Monthly Weather Review, 145, 2575–2595, 2017.

McTaggart-Cowan, R., Davies, E. L., Fairman, J. G., Galarneau, T. J., and Schultz, D. M.: Revisiting the 26.5° C sea surface temperature threshold for tropical cyclone development, Bulletin of the American Meteorological Society, 96, 1929–1943, 2015.

845 Miglietta, M., Laviola, S., Malvaldi, A., Conte, D., Levizzani, V., and Price, C.: Analysis of tropical-like cyclones over the Mediterranean Sea through a combined modeling and satellite approach, Geophysical Research Letters, 40, 2400–2405, 2013.

Miglietta, M., Cerrai, D., Laviola, S., Cattani, E., and Levizzani, V.: Potential vorticity patterns in Mediterranean "hurricanes", Geophysical Research Letters, 44, 2537–2545, 2017.

Miglietta, M. M. and Rotunno, R.: Development mechanisms for Mediterranean tropical-like cyclones (medicanes), Quarterly Journal of the

850 Royal Meteorological Society, 145, 1444–1460, 2019.

Miglietta, M. M., Moscatello, A., Conte, D., Mannarini, G., Lacorata, G., and Rotunno, R.: Numerical analysis of a Mediterranean 'hurricane' over south-eastern Italy: Sensitivity experiments to sea surface temperature, Atmospheric research, 101, 412–426, 2011.

Miglietta, M. M., Mastrangelo, D., and Conte, D.: Influence of physics parameterization schemes on the simulation of a tropical-like cyclone in the Mediterranean Sea, Atmospheric Research, 153, 360–375, 2015.

855 Mogensen, K., Keeley, S., and Towers, P.: Coupling of the NEMO and IFS models in a single executable, ECMWF Reading, United Kingdom, 2012.

Montani, A., Cesari, D., Marsigli, C., and Paccagnella, T.: Seven years of activity in the field of mesoscale ensemble forecasting by the COSMO-LEPS system: main achievements and open challenges, Tellus A: Dynamic Meteorology and Oceanography, 63, 605–624, 2011.

Moscatello, A., Marcello Miglietta, M., and Rotunno, R.: Observational analysis of a Mediterranean 'hurricane' over south-eastern Italy, Weather, 63, 306, 2008.

Munsell, E. B., Zhang, F., and Stern, D. P.: Predictability and dynamics of a nonintensifying tropical storm: Erika (2009), Journal of the atmospheric sciences, 70, 2505–2524, 2013.

Nastos, P., Papadimou, K. K., and Matsangouras, I.: Mediterranean tropical-like cyclones: Impacts and composite daily means and anomalies of synoptic patterns, Atmospheric Research, 208, 156–166, 2018.

Ollinaho, P., Lock, S.-J., Leutbecher, M., Bechtold, P., Beljaars, A., Bozzo, A., Forbes, R. M., Haiden, T., Hogan, R. J., and Sandu, I.: Stochastically Perturbed Parametrizations (SPP)-representing model uncertainties on the process-level, in: EGU General Assembly Conference Abstracts, p. 17706, 2017a.

Ollinaho, P., Lock, S.-J., Leutbecher, M., Bechtold, P., Beljaars, A., Bozzo, A., Forbes, R. M., Haiden, T., Hogan, R. J., and Sandu, I.: Towards process-level representation of model uncertainties: stochastically perturbed parametrizations in the ECMWF ensemble, Quarterly Journal of the Royal Meteorological Society, 143, 408–422, 2017b.

Palmer, T. N., Buizza, R., Doblas-Reyes, F., Jung, T., Leutbecher, M., Shutts, G. J., Steinheimer, M., and Weisheimer, A.: Stochastic parametrization and model uncertainty, 2009.

Pantillon, F., Chaboureau, J.-P., Mascart, P., and Lac, C.: Predictability of a Mediterranean tropical-like storm downstream of the extratropical transition of Hurricane Helene (2006), Monthly Weather Review, 141, 1943–1962, 2013.

Picornell, M., Campins, J., and Jansà, A.: Detection and thermal description of medicanes from numerical simulation, Natural Hazards and Earth System Sciences, 14, 1059–1070, 2014.

Portmann, R., González-Alemán, J. J., Sprenger, M., and Wernli, H.: How an uncertain short-wave perturbation on the North Atlantic wave guide affects the forecast of an intense Mediterranean cyclone (Medicane Zorbas), Weather and Climate Dynamics, 1, 597–615, 2020.

Pytharoulis, I.: Analysis of a Mediterranean tropical-like cyclone and its sensitivity to the sea surface temperatures, Atmospheric Research, 208, 167–179, 2018.

Pytharoulis, I., Craig, G. C., and Ballard, S. P.: The hurricane-like Mediterranean cyclone of January 1995, Meteorological Applications: A journal of forecasting, practical applications, training techniques and modelling, 7, 261–279, 2000.

Rabier, F., Järvinen, H., Klinker, E., Mahfouf, J.-F., and Simmons, A.: The ECMWF operational implementation of four-dimensional variational assimilation. I: Experimental results with simplified physics, Quarterly Journal of the Royal Meteorological Society, 126, 1143–1170, 2000.

Ragone, F., Mariotti, M., Parodi, A., Von Hardenberg, J., and Pasquero, C.: A climatological study of western mediterranean medicanes in numerical simulations with explicit and parameterized convection, Atmosphere, 9, 397, 2018.

Rasmussen, E. and Zick, C.: A subsynoptic vortex over the Mediterranean with some resemblance to polar lows, Tellus A, 39, 408–425, 1987.

Raveh-Rubin, S. and Flaounas, E.: A dynamical link between deep Atlantic extratropical cyclones and intense Mediterranean cyclones, Atmospheric Science Letters, 18, 215–221, 2017.

Ricchi, A., Miglietta, M. M., Bonaldo, D., Cioni, G., Rizza, U., and Carniel, S.: Multi-physics ensemble versus atmosphere–ocean coupled model simulations for a tropical-like cyclone in the Mediterranean Sea, Atmosphere, 10, 202, 2019.

Romero, R. and Emanuel, K.: Medicane risk in a changing climate, Journal of Geophysical Research: Atmospheres, 118, 5992–6001, 2013.

895 Tiedtke, M.: A comprehensive mass flux scheme for cumulus parameterization in large-scale models, Monthly weather review, 117, 1779–1800, 1989.

Tiedtke, M.: Representation of clouds in large-scale models, Monthly Weather Review, 121, 3040–3061, 1993.

Torn, R. D. and Cook, D.: The role of vortex and environment errors in genesis forecasts of Hurricanes Danielle and Karl (2010), Monthly weather review, 141, 232–251, 2013.

900 Vich, M., Romero, R., and Brooks, H.: Ensemble prediction of Mediterranean high-impact events using potential vorticity perturbations. Part I: Comparison against the multiphysics approach, Atmospheric research, 102, 227–241, 2011.

Yanai, M., Esbensen, S., and Chu, J.-H.: Determination of bulk properties of tropical cloud clusters from large-scale heat and moisture budgets, Journal of Atmospheric Sciences, 30, 611–627, 1973.

Zhang, W., Villarini, G., Vecchi, G. A., and Murakami, H.: Rainfall from tropical cyclones: high-resolution simulations and seasonal fore-
905 casts, Climate dynamics, 52, 5269–5289, 2019.

Zhang, W., Villarini, G., Scoccimarro, E., and Napolitano, F.: Examining the precipitation associated with medicanes in the high-resolution ERA-5 reanalysis data, International Journal of Climatology, 41, E126–E132, 2021.

Zimbo, F., Ingemi, D., and Guidi, G.: The tropical-like cyclone "ianos" in September 2020, Meteorology, 1, 29–44, 2022.